

***Vortex sound with special reference to  
vortex rings: theory, computer  
simulations, and experiments***

by

**Tsutomu Kambe**

reprinted from

*international journal of*



***aeroacoustics***

***volume 9 · number 1 & 2 · 2010***

***published by MULTI-SCIENCE PUBLISHING CO. LTD.,***

***5 Wates Way, Brentwood, Essex, CM15 9TB UK***

***E-MAIL: [mscience@globalnet.co.uk](mailto:mscience@globalnet.co.uk)***

***WEBSITE: [www.multi-science.co.uk](http://www.multi-science.co.uk)***

# ***Vortex sound with special reference to vortex rings: theory, computer simulations, and experiments***

**Tsutomu Kambe**

*Higashi-yama 2-11-3, Meguro-ku, Tokyo, 153-0043, Japan  
kambe@ruby.dti.ne.jp*

*Received October 23, 2008; Revised March 1, 2009; Accepted for publication March 7, 2009*

## **ABSTRACT**

This is a review paper on vortex sound with special reference to vortex rings and sound emission detected in experimental tests. Any unsteady vortex motion excites acoustic waves. From the fundamental conservation equations of mass, momentum and energy of fluid flows, one can derive a wave equation of *aerodynamic sound*. The wave equation of acoustic pressure can be reduced to a compact form, called the equation of vortex sound. This equation predicts sound generation by unsteady vortex motions. On the other hand, based on the matched asymptotic expansion (using the multipole expansions), one can derive a formula of wave pressure excited by time-dependent vorticity field localized in space.

The theoretical predictions are compared with experimental observations and direct computer simulations. The systems considered are, head-on collision or oblique collision of two vortex rings, vortex-cylinder interaction, vortex-edge interaction, and others. Scaling laws of the pressure of emitted sound are predicted by the theory and compared with experimental observations. Comparison between theories and observations shows excellence of the theoretical predictions. Direct numerical simulations are reviewed briefly for sound generation by collisions of two vortex rings and that by a cylinder immersed in a uniform stream (*aeolian tones*). Vortex sound in superfluid is also reviewed about experimental observations and computational studies on the basis of the Gross-Pitaevski equation.

## **1. INTRODUCTION**

Any unsteady vortex motion can excite acoustic waves. Physical idea is as follows. Suppose that there exists unsteady fluid flow whose vorticity distribution is localized in space at any time  $t$ , with its length scale denoted by  $l$ . The vorticity field  $\omega$  induces unsteady velocity field  $v$ , whose representative magnitude is denoted by  $u$ . It is important to recognize that the divergence of  $v$  (*i.e.*  $\text{div } v$ ) is non-zero generically by a nonlinear mechanism (*e.g.* see Appendix). In other words, a longitudinal component is excited almost at any point and any time, although it is of second order of  $u$ . The above flow may be called a vortex motion, and the vortex motion drives acoustic waves, called the *vortex sound*. Present article reviews mechanisms of vortex sound at fundamental

levels from theory, experiments and direct computer simulations. Main consideration is focused on experimental verification of the theory by means of experiments using vortex rings and simplified vortex models for mathematical analysis. At the end of this paper, an introductory account is given to sound emission by motion of super-fluid vortices.

Theory of aerodynamic sound was formulated by Lighthill (1952) [42]. This is a reformulation of the basic conservation equations of aerodynamics, resulting in a wave equation. This equation predicts the well-known  $w^8$ -law, namely the acoustic power emitted by a turbulent jet of representative flow speed  $u$  is proportional to  $w^8$ . Recent review of aeroacoustics of subsonic jets is given by Jordan and Gervais (2008) [25] for experiments, modellings and simulations.

Suppose that there exists an unsteady flow field characterized by a time scale  $\tau = l/u$ . Then, the flow field causes a wave field scaled on the length  $\lambda = c\tau$  in its surrounding space, where  $c$  is the sound speed in the undisturbed medium at rest. A Mach number of the flow may be defined by  $M = u/c$ . By the assumption that  $M$  is much less than unity,

$$M \equiv u/c \ll 1,$$

the whole space is separated into two: a space of *inner* source flow and that of *outer* field of wave propagation, because the wave scale  $\lambda = l/M$  is much larger than the scale  $l$  of the source flow. Theory of vortex sound can be developed under these circumstances. This is the framework of mathematical formulation given in this paper, although it is not necessary in general [17, 18].

Reformulating the Lighthill's theory of aerodynamic sound, the sound source was identified with a term of the form  $\rho_0 \operatorname{div}(\boldsymbol{\omega} \times \boldsymbol{v})$  at low  $M$ , first by Powell (1964) [58] and later by Howe (1975) [18], where  $\rho_0$  is the undisturbed fluid density. As shown in §2.4, the wave equation for the acoustic pressure  $p$  is written as

$$c^{-2} \partial_t^2 p - \nabla^2 p = \rho_0 \operatorname{div}(\boldsymbol{\omega} \times \boldsymbol{v}), \quad (\partial_t = \partial/\partial t) \quad (1)$$

in the limit of  $M \rightarrow 0$ . This can be derived as an approximation from the basic conservation equations. These formulations are described in §2 (general) and in §3 (vortex sound in an inviscid fluid). Section 3 describes a general formulation of multipole expansions for wave generation on the basis of matched asymptotic expansions by Kambe *et al.* (1993) [34].

Experimental detection of the vortex sound was attempted first by Kambe & Minota (1983) [32] for the sound emitted by head-on collision of two vortex rings. The detected acoustic signals were compared with theoretically computed wave profiles. This analysis confirmed excellent agreement between the theory and experiment, and clarified that generated sound field is dominated by *quadrupolar* waves.

Subsequently, experimental investigations were carried out for sound generation by oblique collision of two vortex rings [34], described in §4, which is a three-dimensional phenomenon. In this oblique collision, there is a process of reconnection of vortex lines at the time of collision. This is investigated in particular by a new

approach of vorticity-potential method by Ishii *et al.* (1998) [22] to solve numerically the three-dimensional viscous vorticity equation.

Section 5 presents sound emission by vortex-body interaction. General mathematical formulation is first presented for the wave generated by vortex-body interaction. It is found that the acoustic wave profile can be related to a time derivative of volume flux (through the vortex ring) of an imaginary potential flow around the body (something like the Faraday's law in the electromagnetism), characterized as a *dipolar* emission. Experimental tests were carried out for some particular arrangements of vortex-body system such as a vortex motion interacting with a circular cylinder [46], or with a sphere [47]. Section 7 describes sound generation by a vortex interacting with a sharp edge [33]. The wave is characterized by *cardioid* profiles. All the wave emissions were detected experimentally. The experimental tests were successful in showing remarkable agreement between the theory and experiment, summarized in [27]. In the mathematical analyses of the vortex-body interaction, vortex shedding is disregarded. Consideration is restricted only to the interaction of a vortex ring with a solid body in the above cases. Even though that is the case, the agreement is remarkable in the cases of experimental tests described above.

Oscillations of vortex core of a vortex ring emit sound waves [36]. A review article by Kopiev and Chernyshev [35] describes this phenomenon together with some experimental investigations [62, 63] of sound radiated from a turbulent vortex ring. Remarkably new aspect is the recent study of superfluidity of atomic Bose-Einstein condensates (BEC), in which quantized circulation (called a quantized vortex) is supported. It is found that sound waves are emitted by accelerating motion of a quantum vortex. [4]

Recent innovative development of high-speed computers together with high performance computation codes enabled a research area of computational aeroacoustics (CAA), *i.e.* direct computer simulations of vortex sound by solving the Navier-Stokes equation for a compressible fluid. These simulations based on first-principles give an insight into the mechanisms of sound generation directly. Direct computation of the whole field, including both source flow and wave field generated, is practically important because it allows detailed look at any flow variable of interest. However, reliability of the computation code must be tested by experimental data. The above experimental studies of vortex sound (providing detected acoustic data) served an essential role to test the performance of CAA, by comparing computationally generated data with the observed signals [23, 52, 53].

Recent progress in computational aeroacoustics is reviewed by Colonius and Lele (2004) [5], where critical assessments are made for computation codes. This describes among others significant progress made in the use of LES (Large-eddy simulation) for jet noise predictions. Another recent review of CAA is also given by Wang *et al.* (2006) [61] for flow noise prediction by discussing both numerical methods and flow simulation techniques.

Direct numerical simulation (DNS) of vortex sound was carried out by Inoue, Hattori & Sasaki (2000) [23] for axisymmetric problem of collision of two vortex rings. The DNS data were compared with the results of [32] and [45]. Three-dimensional computer simulations of oblique collision of two vortex rings were carried out by

Nakashima, Hatakeyama & Inoue [53] and Nakashima [52] and compared with the experiment of Kambe *et al.* [34].

The same computational technique can be applied to various problems of aeroacoustics. In particular, DNS study of mechanism of an aeolian tone was made by Inoue & Hatakeyama (2002) [24], where wave field was obtained by computing the whole flow field around a circular cylinder immersed in a uniform flow. This clarifies a dipolar nature of generated sound field. Section 6 describes this subject as a typical example of sound generation by a body in a flow. This is in clear contrast with the quadrupolar field generated by vortices in the absence of solid bodies. In this problem, the generated sound waves are influenced by convective effect by the source flow.

In superfluid too, vortex motions are found to generate sound waves. Section 8 describes the vortex sound in superfluid. A quantum-mechanic model of quantized vortex lines is provided by a nonlinear Schrödinger equation, which is also called the Gross-Pitaevskii (GP) equation in the context of BEC. The GP equation predicts excitation of acoustic waves by vortex motions (*e.g.* [4]). This equation is also a fluid dynamical model capable of describing vortex reconnection. Sound emission due to superfluid vortex reconnection was also studied by solving the GP equation [43].

## 2. THEORY OF AERODYNAMIC SOUND AND VORTEX SOUND

The fluid is characterized by the density  $\rho$ , pressure  $p$  and enthalpy  $h$ . The undisturbed state is assumed to have uniform density  $\rho_0$ , pressure  $p_0$  and entropy  $s_0$ , and that  $\rho'$  and  $p'$  denote deviations from the uniform values. The shear viscosity  $\mu$ , kinematic viscosity  $\nu = \mu/\rho_0$ , thermal conductivity  $k$  and sound speed  $c = \sqrt{(\partial p/\partial \rho)_s} \Big|_{\rho=\rho_0, p=p_0}$  are assumed to be constant.

### 2.1. Lighthill's equation of aerodynamic sound

We first consider the fundamental conservation equations of mass and momentum of a viscous fluid, which are written as

$$\frac{\partial}{\partial t} \rho + \frac{\partial}{\partial x_i} (\rho v_i) = 0, \quad (2)$$

$$\frac{\partial}{\partial t} (\rho v_i) + \frac{\partial}{\partial x_k} \Pi_{ik} = 0, \quad (3)$$

$$\Pi_{ik} = \rho v_i v_k + (p - p_0) \delta_{ik} - \sigma_{ik}, \quad (4)$$

where  $v_i$  ( $i = 1, 2, 3$ ) are the components of fluid velocity with respect to the cartesian space coordinates  $x_i$ ,  $\Pi_{ik}$  the stress tensor, and  $\sigma_{ij}$  the viscous stress tensor defined by

$$\sigma_{ik} = \mu e_{ik}, \quad e_{ik} = \partial v_i / \partial x_k + \partial v_k / \partial x_i - \frac{2}{3} \delta_{ik} \partial v_l / \partial x_l. \quad (5)$$

A constant term  $\rho_0 \delta_{ik}$  is added to  $\Pi_{ik}$ , which is introduced for convenience and has no influence in the momentum equation. Differentiating (2) with respect to  $t$  and taking divergence of (3), one can eliminate the common term of the form  $\partial_t \partial(\rho v_i) / \partial x_i$  from the two equations.

Thus, the following *Lighthill's equation* is obtained for  $\rho'$ :

$$(\nabla^2 - c^{-2} \partial_t^2) \rho' = -\frac{1}{c^2} \frac{\partial}{\partial x_i} \frac{\partial}{\partial x_k} T_{ik}, \quad \equiv -S(\mathbf{x}, t), \quad (6)$$

( $\rho' = \rho - \rho_0$ ,  $p' = p - p_0$ ), where  $T_{ik}$  is the Lighthill's tensor defined by

$$T_{ik} = \Pi_{ik} - c^2 \rho' \delta_{ik} = \rho v_i v_k + (p' - c^2 \rho') \delta_{ik} - \sigma_{ik}. \quad (7)$$

The first term  $\nabla^2 \rho'$  on the left of (6) is newly introduced, which is cancelled by the term  $-c^2 \rho' \delta_{ik}$  in  $T_{ik}$  on the right side.

The expression (6) is transformed immediately to the following integral form (by the standard theory of wave equation):

$$\rho'(\mathbf{x}, t) = \frac{1}{4\pi} \int \frac{S(\mathbf{y}, t_r)}{|\mathbf{x} - \mathbf{y}|} d^3 \mathbf{y}, \quad t_r = t - \frac{|\mathbf{x} - \mathbf{y}|}{c}, \quad (8)$$

$$= \frac{1}{4\pi c^2} \frac{\partial}{\partial x_i} \frac{\partial}{\partial x_k} \int \frac{T_{ik}(\mathbf{y}, t_r)}{|\mathbf{x} - \mathbf{y}|} d^3 \mathbf{y}, \quad (9)$$

where  $t_r$  is the retarded time, expressing time delay due to wave propagation from the source position at  $\mathbf{y}$  to the observation station at  $\mathbf{x}$ . The last expression (9) states that the directivity of the wave density  $\rho'(\mathbf{x}, t)$  is characterized by *quadrupolar* waves, implied by the second spatial derivative in front of the integral sign. From this integral expression, Lighthill [42] derived the well-known  $u^8$ -law for the acoustic power output from turbulent jets. This power law is a consequence of the fact that in free turbulent flow there are no external forces allowing to support a dipole and that at low Mach number monopoles related to entropy production can be neglected.<sup>1</sup>

## 2.2. Equations of an inviscid fluid

Motion of an inviscid fluid is governed by the Euler equation,

$$\partial_t \mathbf{v} + (\mathbf{v} \cdot \nabla) \mathbf{v} = -\nabla h, \quad \nabla h = \frac{1}{\rho} \nabla p, \quad (10)$$

when the fluid is also *homotropic*, where  $\mathbf{v} = (v_i)$  and  $\nabla = (\partial / \partial x_i)$ , together with the equation of continuity (2). The second term  $(\mathbf{v} \cdot \nabla) \mathbf{v}$  can be rewritten by the following vector identity:

<sup>1</sup>This comment is suggested by one of the referees.

$$(\mathbf{v} \cdot \nabla) \mathbf{v} = \boldsymbol{\omega} \times \mathbf{v} + \nabla(v^2/2), \quad (11)$$

Using this, the equation for the vorticity  $\boldsymbol{\omega} = \nabla \times \mathbf{v}$  is obtained from (10) as

$$\partial_t \boldsymbol{\omega} + \nabla \times (\boldsymbol{\omega} \times \mathbf{v}) = 0. \quad (12)$$

### 2.3. Reformulation of the equation of aerodynamic sound

Conservation equations of mass, momentum and energy of a viscous fluid can be rewritten as follows (Kambe & Minota [32], Appendix A):

$$\nabla \cdot \mathbf{v} = -\frac{1}{\rho} \frac{D\rho}{Dt}, \quad (13)$$

$$\frac{\partial \mathbf{v}}{\partial t} + \mathbf{L} + \nabla \left( \frac{1}{2} \mathbf{v}^2 \right) = -\frac{1}{\rho} \nabla p + \nu \nabla \cdot \underline{\underline{e}}, \quad (14)$$

$$T \frac{Ds}{Dt} = \nu \underline{\underline{e}} : \nabla \mathbf{v} + k \nabla^2 T, \quad (15)$$

where  $T$  and  $s$  are the temperature and entropy (per unit mass) respectively,  $D/Dt$  is the convective derivative  $\partial_t + \mathbf{v} \cdot \nabla$ , and

$$\mathbf{L} = \boldsymbol{\omega} \times \mathbf{v} \quad (16)$$

$$\underline{\underline{e}} \equiv (e_{ik}), \quad \nabla \cdot \underline{\underline{e}} = (\partial/\partial x_k) e_{ik}, \quad \underline{\underline{e}} : \nabla \mathbf{v} = e_{ik} (\partial/\partial x_i) v_k.$$

Using thermodynamic relations, variations of pressure  $p$  and density  $\rho$  can be expressed in terms of the entropy  $s$  and enthalpy  $h$  as

$$\frac{1}{\rho} dp = dh - T ds, \quad \frac{1}{\rho} d\rho = \frac{1}{c^2} dh - \left( \frac{T}{c^2} + \frac{1}{C_p} \right) ds, \quad (17)$$

where  $C_p$  is the specific heat at constant pressure. The second relation of (17) is derived from the relation  $d\rho = c^{-2} dp + (\rho/C_p) ds$  for an ideal gas by substituting the first relation to  $dp$ . The equation (14) is transformed to

$$\nabla \left( h + \frac{1}{2} v^2 \right) + \frac{\partial \mathbf{v}}{\partial t} - T \nabla s = -\mathbf{L} + \nu \nabla \cdot \underline{\underline{e}}, \quad (18)$$

by eliminating  $\rho^{-1} \nabla p$  with using the first of Eq. (17). Similarly, with use of the second equation of (17), Eq. (13) is written as

$$\nabla \cdot \mathbf{v} = -\frac{1}{c^2} \frac{D}{Dt} h + \left( \frac{T}{c^2} + \frac{1}{c_p} \right) \frac{D}{Dt} s. \quad (19)$$

Taking divergence of (18), we have

$$\nabla^2 (h + \frac{1}{2} v^2) + \frac{\partial}{\partial t} \nabla \cdot \mathbf{v} - \nabla \cdot (T \nabla s) = -\nabla \cdot \mathbf{L} + \nu \nabla \nabla : \underline{e}, \quad (20)$$

where  $\nabla \nabla : \underline{e} = (\partial/\partial x_i)(\partial/\partial x_k)e_{ik} = \frac{4}{3} \nabla^2 (\nabla \cdot \mathbf{v})$ . The term  $(\partial/\partial t) \nabla \cdot \mathbf{v}$  of Eq. (20) can be expressed in terms of  $h$  and  $s$  by using Eq. (19), in which  $(\mathbf{v} \cdot \nabla)h$  can be eliminated by using the equation obtained with taking scalar product of  $\mathbf{v}$  and Eq. (18). Thus, we find the following inhomogeneous wave equation:

$$(\nabla^2 - c^{-2} \partial_t^2)(h + \frac{1}{2} v^2) = -F(\mathbf{x}, t), \quad (21)$$

$$\begin{aligned} F(\mathbf{x}, t) = & \nabla \cdot \mathbf{L} + c^{-2} \partial_t^2 v^2 + c^{-2} \partial_t [(\mathbf{v} \cdot \nabla) \frac{1}{2} v^2] \\ & + \frac{\partial}{\partial t} \left[ \left( \frac{T}{c^2} + \frac{1}{c_p} \right) \frac{Ds}{Dt} \right] + \nabla \cdot (T \nabla s) - \nu c^{-2} \partial_t [\mathbf{v} \nabla : \underline{e}] \\ & + \frac{4}{3} \nu \nabla^2 (\nabla \cdot \mathbf{v}). \end{aligned} \quad (22)$$

Obviously, the equation (21) is a wave equation for the variable  $h + \frac{1}{2} v^2$  where the source term  $F(\mathbf{x}, t)$  is defined by Eq. (22). The variable  $h + \frac{1}{2} v^2$  was first taken into account in the theory of vortex sound by Howe [17]. This is another equation of *aerodynamic sound* for a viscous fluid. Just like the previous case to obtain the integral expression (8) from (6), the equation (21) is transformed to the following integral form:

$$[h + \frac{1}{2} v^2](\mathbf{x}, t) = \frac{1}{4\pi} \int \frac{F(\mathbf{y}, t_r)}{|\mathbf{x} - \mathbf{y}|} d^3 \mathbf{y}. \quad (23)$$

#### 2.4. Equation of vortex sound

Suppose that the vorticity distribution  $\boldsymbol{\omega}(\mathbf{x}, t)$  is *compact*, i.e. localized in space. Then the velocity field  $\mathbf{v}(\mathbf{x}, t)$  induced by the vorticity  $\boldsymbol{\omega}(\mathbf{x}, t)$  has an asymptotic property decaying as  $O(x^{-3})$  in the far field as  $x = |\mathbf{x}| \rightarrow \infty$  (see the last sentence of §3.1). In the far field where deviations from the uniform state is infinitesimal and the wave propagation is regarded as adiabatic (i.e.  $ds = 0$ ), we have  $h + \frac{1}{2} v^2 \rightarrow p'/\rho_0$  from the first of the relations (17) since  $|\mathbf{v}(\mathbf{x})| = O(x^{-3})$ . Then the equation (23) becomes

$$p'(\mathbf{x}, t) = \frac{\rho_0}{4\pi} \int \frac{F(\mathbf{y}, t_r)}{|\mathbf{x} - \mathbf{y}|} d^3 \mathbf{y}, \quad t_r = t - \frac{|\mathbf{x} - \mathbf{y}|}{c}. \quad (24)$$

It is well-known that the rate of viscous dissipation of kinetic energy, denoted by  $K'(t)$ , is given by

$$K'(t) := \frac{d}{dt} \int_V \frac{1}{2} v^2 d^3 \mathbf{y} = -\nu \int_V e_{ik} \frac{\partial v_i}{\partial x_k} d^3 \mathbf{y}. \quad (25)$$

The heat delivered to the fluid in a unit time is equal to the rate of dissipation of kinetic energy, *i.e.*  $-K'(t)$  is equal to the space integral of  $TDs/Dt$ . Using these relations, we can simplify the above expression (24) of acoustic pressure under the viscous action as follows [32, Appendix A]:

$$p'(\mathbf{x}, t) = \frac{\rho_0}{4\pi} \int \frac{\nabla \cdot \mathbf{L}(\mathbf{y}, t_r)}{|\mathbf{x} - \mathbf{y}|} d^3 \mathbf{y} + \frac{\rho_0}{4\pi c^2} (2 - \gamma) \frac{1}{r} K''(t - \frac{r}{c}) \quad (26)$$

$$= -\frac{\rho_0}{4\pi c} \frac{x_i}{r^2} \frac{\partial}{\partial t} \int L_i(\mathbf{y}, t - \frac{r}{c}) d^3 \mathbf{y} + \frac{\rho_0}{4\pi c^2} (2 - \gamma) \frac{1}{r} K''(t - \frac{r}{c}), \quad (27)$$

where  $\mathbf{L} = \boldsymbol{\omega} \times \mathbf{v}$ .

In an ideal fluid where there is no viscous dissipation, the kinetic energy  $K$  is constant. Hence the second term vanishes identically in the above expression (26) (or (27)). Then, the expression (26) implies the following differential equation (using  $p$  instead of  $p'$ ):

$$\frac{1}{c^2} \partial_t^2 p - \nabla^2 p = \rho_0 \nabla \cdot \mathbf{L}, \quad = \rho_0 \operatorname{div}(\boldsymbol{\omega} \times \mathbf{v}), \quad (28)$$

which is called the *equation of vortex sound*. [18, 20, 51]

Based on (28), Möhring [51] succeeded in representing the acoustic pressure  $p'$  in terms of the vorticity  $\boldsymbol{\omega}$  only, and gave a mathematical basis for the term “*vortex sound*”. About ten years earlier, Obermeier [55] found a formula of an acoustic wave emitted by a spinning pair of two 2D vortices. An acoustic wave radiated by head-on collision of two vortex rings was detected experimentally first by Kambe & Minota [32].

In the equation (28), it is assumed that the source vorticity  $\boldsymbol{\omega}(\mathbf{x}, t)$  is compact in space and its representative Mach number  $M$  is sufficiently low. It is remarked that  $p(\mathbf{x}, t)$  satisfies the wave equation (28) (approximately), when  $\mathbf{x}$  is far from a *compact* source at  $\mathbf{y}$ . If the source term  $\rho_0 \operatorname{div}(\boldsymbol{\omega} \times \mathbf{v})$  is evaluated with an incompressible vortex motion, the error would be  $O(M^2)$ . The acoustic waves generated by vortex motion in an ideal fluid is also represented by the first term of Eq. (27).

### 3. MATCHED ASYMPTOTIC EXPANSIONS

The expressions of vortex sound in the previous section can be derived from another formulation, that is the matched asymptotic expansion equivalent to the multipole expansions. This is the subject of this section. As described in the introduction, if the

vorticity field is compact in space and the typical flow Mach number is much less than unity, the whole space is separated into two: a space of *inner* source flow and that of *outer* field of wave propagation, because the wave scale  $\lambda = l/M$  is much larger than scale  $l$  of the source flows. Method of matched expansions (MAE) was applied to the problems of vortex sound first by [55]. The method MAE was developed later in details by various authors [7, 9, 10, 38, 39]. However, the present formulation is different from those, so that full formulation is presented here.

### 3.1. Inner flow region

The *inner flow region* is scaled on  $l$ , and the inner velocity is scaled on  $u$ . Inner dimensionless variables are denoted with a bar:

$$\bar{x}_i = \frac{x_i}{l}, \quad \bar{t} = \frac{t}{\tau}, \quad \bar{p} = \frac{p - p_0}{\rho_0 u^2}, \quad \bar{v}_i = \frac{v_i}{u}, \quad \bar{\nabla} = l \nabla. \quad (29)$$

where  $\tau = l/u$ . Then, the equation (28) is rewritten as

$$\bar{\nabla}^2 \bar{p} = -\overline{\text{div}(\bar{\omega} \times \bar{v})} + O(M^2). \quad (30)$$

The equation of an incompressible fluid is equivalent to neglecting the  $O(M^2)$  terms.

Let us consider a solenoidal velocity field  $\mathbf{v}(\mathbf{x}, t)$  (*i.e.*  $\text{div } \mathbf{v} = 0$ ) induced by a localized vorticity field  $\boldsymbol{\omega}(\mathbf{x}, t)$ , which is given at an initial instant in a bounded domain  $D_0$  of linear dimension  $O(l)$  (*i.e.*  $\boldsymbol{\omega}(\mathbf{x}, 0) = 0$  for  $\mathbf{x}$  not in  $D_0$ ), and stays in a bounded domain  $D_t$  at a subsequent time  $t$ . The  $\boldsymbol{\omega}(\mathbf{x}, t)$  is governed by the vorticity equation (12).

Introducing a vector potential  $\mathbf{A}(\mathbf{x}, t)$ , the solenoidal velocity is represented by

$$\mathbf{v}(\mathbf{x}, t) = \text{curl } \mathbf{A}, \quad \mathbf{A}(\mathbf{x}, t) = \frac{1}{4\pi} \int_{D_t} \frac{\boldsymbol{\omega}(\mathbf{y}, t)}{|\mathbf{x} - \mathbf{y}|} d^3 \mathbf{y}. \quad (31)$$

It can be shown that taking curl of  $\mathbf{v}$  of (31) results in  $\boldsymbol{\omega}$  in the free space. [Note that  $\text{curl}^2 \mathbf{A} = -\nabla^2 \mathbf{A} + \nabla(\nabla \cdot \mathbf{A})$ , and that the Green's function  $G = 1/(4\pi |\mathbf{x} - \mathbf{y}|)$  satisfies (39), and that  $\nabla \cdot \mathbf{A} = 0$  [3, §2.4].]

At large distances  $x \equiv |\mathbf{x}| \gg y \equiv |\mathbf{y}|$  for  $\mathbf{y} \in D_t$ , it is an elementary exercise that we have the following asymptotic expansion:

$$\frac{1}{|\mathbf{x} - \mathbf{y}|} = \frac{1}{x} - y_i \frac{\partial}{\partial x_i} \frac{1}{x} + \frac{1}{2} y_i y_j \frac{\partial^2}{\partial x_i \partial x_j} \frac{1}{x} - \frac{1}{3!} y_i y_j y_k \frac{\partial^3}{\partial x_i \partial x_j \partial x_k} \frac{1}{x} + \dots \quad (32)$$

Outside  $D_t$ , the velocity  $\mathbf{v}$  is irrotational (by the definition of domain  $D_t$ ) and represented by the form  $\mathbf{v} = \text{grad } \Phi$ . According to the formulation of [34], the velocity potential  $\Phi$  associated with the vorticity  $\boldsymbol{\omega}(\mathbf{x}, t)$  is given by the following series expansion at large  $x$ :

$$\Phi(\mathbf{x}, t) = Q_0(\mathbf{x}, t) + Q_i \frac{\partial}{\partial x_i} \frac{1}{x} + Q_{ij} \frac{\partial^2}{\partial x_i \partial x_j} \frac{1}{x} + Q_{ijk} \frac{\partial^3}{\partial x_i \partial x_j \partial x_k} \frac{1}{x} + O(x^{-5}), \quad (33)$$

$$Q_i(t) = \frac{1}{8\pi} \int_{D_t} (\mathbf{y} \times \boldsymbol{\omega})_i d^3 \mathbf{y}, \quad Q_{ij}(t) = -\frac{1}{12\pi} \int_{D_t} y_i (\mathbf{y} \times \boldsymbol{\omega})_j d^3 \mathbf{y}, \quad (34)$$

$$Q_{ijk}(t) = \frac{1}{32\pi} \int_{D_t} (\mathbf{y} \times \boldsymbol{\omega})_i y_j y_k d^3 \mathbf{y}, \quad \dots, \quad (35)$$

where  $Q_0(\mathbf{x}, t)$  is a scalar function of  $\mathbf{x}$  and  $t$  associated with local change of density. The vector  $P_i \equiv 4\pi Q_i$  is the well-known flow impulse. In the absence of external forces and bodies, the impulse  $P_i$  is conserved. The tensor  $Q_{ij}$  is second moments of the vorticity distribution  $\boldsymbol{\omega}(\mathbf{y})$  (satisfying  $Q_{ii} = 0$ ). In §3.4 below,  $Q_{ij}$  will be related to the wave profile generated by vortex motions. In general they depend on the time  $t$ . It will be shown that the excitation of an acoustic wave by a rotational flow (31) is closely related to the time dependence of the coefficients of the multipole expansion (33).

In the context of the vortex sound in an inviscid fluid considered in §2.4, the inner flow field is assumed to be incompressible (and the kinetic energy is conserved). Hence the compressive component  $Q_0$  can be omitted. In this case, the expression (33) without the first term suggests that the magnitude of  $v_i = \partial\Phi/\partial x_i$  is given by  $\partial_i(Q_j \partial_j(1/x)) = O(x^{-3})$  as  $x \rightarrow \infty$ , where  $\partial_i = \partial/\partial x_i$ .

### 3.2. Outer wave region

Next, we consider the space with a much larger scale. Using the scaling length  $\lambda (\gg l)$ , we obtain the following estimate of magnitudes,

$$O\left(\frac{1}{c^2} p_{tt}\right) / O(\nabla^2 p) = \frac{\lambda^2}{c^2 \tau^2} \approx 1.$$

Hence, the two terms on the left hand side of (28) are comparable in magnitudes. In general, the pressure deviation  $p$  (and  $p_{tt}/c^2$  as well) associated with compressible motion decays as  $x^{-1}$ , whereas the velocity  $v_i$  on the right hand side decays like  $O(x^{-3})$  as noted above. Introducing the outer variables defined by

$$\begin{aligned} \hat{x}_i &= \frac{x_i}{\lambda} = M \bar{x}_i, & \hat{t} &= \bar{t} = \frac{t}{\tau}, & M &= l / \lambda, \\ \hat{p} &= \frac{p - p_0}{\rho_0 u^2}, & \hat{v}_i &= \frac{v_i}{u}, & \hat{\nabla} &= \lambda \nabla. \end{aligned} \quad (36)$$

it is found that the equation (21) reduces to

$$\frac{\partial^2}{\partial \hat{t}^2} \hat{p} - \hat{\nabla}^2 \hat{p} = 0, \tag{37}$$

neglecting  $O(M^{4+2\beta})$  terms relative to those retained. (From (21), the equations (26) or (28) are derived for the acoustic pressure regardless of the division of inner and outer regions.) This is a wave equation, implying that there exists a region of wave propagation at large distances. The compressible component of velocity, which is given by  $p/c\rho_0$  in the linear theory of infinitesimal sound wave, decays as  $ul M^{1+\beta} x^{-1}$ , where  $\beta = 1.0$  (dipolar wave), 2.0 (quadrupolar wave), and 0.5 (wave generated by an edge). See [26].

### 3.3. Pressures of inner and outer regions

#### 3.3.1. Inner region

To the leading order, the flow in the inner region is governed by the incompressible equation of motion, and the pressure of incompressible flows is determined by

$$\nabla^2 p = -\rho_0 \nabla \cdot \mathbf{L}, \tag{38}$$

according to (30) (with using original dimensional variables). This is a Poisson type equation for  $p$ . Introducing the Green's function  $G(\mathbf{x}, \mathbf{y})$  satisfying

$$\nabla_x^2 G(\mathbf{x}, \mathbf{y}) = -\delta(\mathbf{x} - \mathbf{y}), \tag{39}$$

where  $\nabla_x$  is a nabla operator with respect to the variable  $\mathbf{x} = (x_i)$ , we obtain the following integral representation for the inner pressure  $p_1$ ,

$$p_1 := p - p_0 = \rho_0 \int G(\mathbf{x}, \mathbf{y}) \nabla_{\mathbf{y}} \cdot \mathbf{L}(\mathbf{y}, t) d^3 \mathbf{y}. \tag{40}$$

in unbounded space, where  $G(\mathbf{x}, \mathbf{y})$  is the free space Green's function given below.

If there is a solid body, boundary conditions are to be imposed on the body surface  $S$ :

$$\mathbf{n} \cdot \mathbf{v} = 0, \quad \text{on } S, \tag{41}$$

$$\mathbf{n} \cdot \nabla_{\mathbf{y}} \mathbf{G} = 0, \quad \text{for } \mathbf{y} \text{ on } S, \tag{42}$$

where  $\mathbf{n}$  is a unit normal to  $S$ . Then, the inner pressure is represented by

$$p_1(\mathbf{x}, t) = -\rho_0 \int \mathbf{L}(\mathbf{y}, t) \cdot \nabla_{\mathbf{y}} G(\mathbf{x}, \mathbf{y}) d^3 \mathbf{y}. \tag{43}$$

It is remarkable that this integral representation is valid whether a solid body is present or not [26].

### 3.3.2. Outer region

The outer region is governed by the wave equation (37). With using an arbitrary function  $a(\hat{t})$  and  $\hat{x} = |\hat{x}|$ , a function of the form  $\hat{x}^{-1}a(\hat{t} - \hat{x})$  is a solution of the equation (37). Its derivative, obtained by differentiating arbitrary times with respect to the space coordinates  $\hat{x}_i$ , is a solution as well. Thus the acoustic pressure  $p_O = p - p_0$  in the outer region is represented in the form of multipole expansions:

$$p_O(\mathbf{x}, t) = \frac{A_0(\hat{t} - \hat{x})}{\hat{x}} + \frac{\partial}{\partial \hat{x}_i} \frac{A_i(\hat{t} - \hat{x})}{\hat{x}} + \frac{\partial^2}{\partial \hat{x}_i \partial \hat{x}_j} \frac{A_{ij}(\hat{t} - \hat{x})}{\hat{x}} + \dots, \quad (44)$$

[10], where  $\hat{t} - \hat{x} = (t - x/c)\tau$  is the retarded time in the outer variables. The functions  $A_0(\hat{t})$ ,  $A_i(\hat{t})$ ,  $A_{ij}(\hat{t})$ , ... (with the dimension of pressure) are unknowns to be determined by matching to the inner pressure  $p_I$ . In other words, the pressure  $p_O$  represents the acoustic waves generated by vortex motion if the functions  $A_0(\hat{t})$ ,  $A_i(\hat{t})$ ,  $A_{ij}(\hat{t})$ , ... are expressed in terms of the vorticity  $\boldsymbol{\omega}(\mathbf{x}, t)$ .

### 3.3.3. Matching

Matching of the two expressions  $p_I(\mathbf{x}, t)$  and  $p_O(\mathbf{x}, t)$  is carried out in an intermediate region, on the basis of the method of matched asymptotic expansions. The outer pressure  $p_O(\hat{x}, \hat{t})$  is expanded with the limit as  $\hat{x} \rightarrow 0$ , whereas the inner pressure  $p_I(\bar{x}, \bar{t})$  is expanded with the outer limit as  $\bar{x} \rightarrow \infty$ . The matching requires that leading terms of both expansions match to each other in an (overlapping) intermediate region. By this matching [34], the functions  $A_0(\hat{t})$ ,  $A_i(\hat{t})$ ,  $A_{ij}(\hat{t})$ , ... are represented with the vorticity  $\boldsymbol{\omega}(\mathbf{x}, t)$ . Then, the wave  $p_O(\mathbf{x}, t)$  of (44) is called the *vortex sound*.

## 3.4. Vortex sound in free space

In this section, we consider the vortex sound in free space, *i.e.* in the absence of external bodies (nor forces). Green's function in free space is given by

$$G(\mathbf{x}, \mathbf{y}) = \frac{1}{4\pi|\mathbf{x} - \mathbf{y}|}, \quad (45)$$

which is to be substituted in (43). It is assumed that the point of observation  $\mathbf{x}$  is at large distances from the point  $\mathbf{y}$  located within the vortex flow, *i.e.* it is assumed that  $x \gg y$  where  $y = O(l)$ . Using the expansion (32), one can find the following expansion [26]:

$$\nabla \mathbf{y} G(\mathbf{x}, \mathbf{y}) = -\frac{1}{4\pi} \nabla \frac{1}{x} + \nabla \mathbf{y} \times \mathbf{g} + O(x^{-4}), \quad (46)$$

$$\mathbf{g}(\mathbf{x}, \mathbf{y}) := \frac{1}{4\pi x^5} (\mathbf{x} \cdot \mathbf{y})(\mathbf{x} \times \mathbf{y}). \quad (47)$$

When (46) is substituted into (43), it is readily seen that the contribution from the first term disappears. (The factor  $\nabla(1/x)$  can be taken out of the integral, and note that we have  $L_i = (\boldsymbol{\omega} \times \mathbf{v})_i = \partial_j(v_i v_j - \frac{1}{2}v^2 \delta_{ij})$  by using (11) and  $\partial_j v_j = 0$ .) Regarding the second term, integration by parts transforms the integrand into the form  $-\rho_0(\nabla \times \mathbf{L}) \cdot \mathbf{g}$ . Noting  $\mathbf{L} = \boldsymbol{\omega} \times \mathbf{v}$ , we find that  $\nabla \times \mathbf{L} = -\partial_t \boldsymbol{\omega}$  from (12). Thus, the inner pressure is reduced to the expression,

$$\begin{aligned} p_1(\mathbf{x}, t) &= \rho_0 \frac{d}{dt} \int \boldsymbol{\omega}(\mathbf{y}, t) \cdot \mathbf{g}(\mathbf{x}, \mathbf{y}) d^3 \mathbf{y} + O(x^{-4}) \\ &= -\rho_0 Q'_{ij}(t) \frac{\partial^2}{\partial x_i \partial x_j} \frac{1}{x} + O(x^{-4}), \end{aligned} \quad (48)$$

where the prime denotes differentiation with respect to the time  $t$ , and the tensor  $Q_{ij}$  defined by (34) is rewritten here:

$$Q_{ij}(t) = -\frac{1}{12\pi} \int_{\mathcal{D}} y_i (\mathbf{y} \times \boldsymbol{\omega})_j d^3 \mathbf{y}. \quad (49)$$

It is remarkable that the factor  $(\partial^2/\partial x_i \partial x_j)x^{-1}$  of the leading term denotes quadrupole potentials with time-dependent coefficient  $Q'_{ij}(t)$ .

The matching procedure of §3.3.3 leads to the expression of the outer pressure from (48):

$$p_O(\mathbf{x}, t) = -\rho_0 \frac{\partial^2}{\partial x_i \partial x_j} \frac{Q'_{ij}(t - x/c)}{x}.$$

This is the pressure formula of the vortex sound [26], since  $Q'_{ij}(\hat{t} - \hat{x})$  is approximated by  $Q'_{ij}(\hat{t})$  in the inner region as  $\hat{x} \rightarrow 0$ . In the far field as  $\hat{x} \rightarrow \infty$ , the pressure takes the following simpler form,

$$p_F(\mathbf{x}, t) = -\frac{\rho_0}{c^2} \frac{x_i x_j}{x^3} Q'''_{ij}(t - x/c). \quad (50)$$

It is obvious that this has the property of a *quadrupolar* wave. [Note: Operating  $\partial_i$  to the factor  $1/x$ ; gives a higher order term of  $O(1/x^2)$ , which was neglected.]

From (50), scaling law of the quadrupolar wave is deduced in the following way. Using the length scale  $l$ , the vorticity scale  $\omega = u/l$  and the time scale  $\tau = l/u$ , the tensor  $Q_{ij}$  is normalized by  $ul^4$ , and hence  $Q'''_{ij}$  by  $ul^4/\tau^3 = u^4 l$ . Thus we find the scaling law of pressure of the quadrupole sound, denoted by  $p_Q$ , as (using  $r$  in place of  $x$ )

$$p_Q \sim \frac{\rho_0}{c^2} \frac{1}{r} u^4 l = \frac{\rho_0 u^4}{c^2} \frac{1}{r}. \quad (51)$$

The sound intensity  $I_Q$  is given by  $p_Q^2/\rho_0 c$ . Hence we obtain the well-known law:  $I_Q \sim (\rho_0 u^8/c^5)(l/r)^2 \propto u^8$ . [42]

### 3.5. Head-on collision of two vortex rings

Vortex sound generated by head-on collision of two vortex rings was investigated mathematically by Kambe & Minota [31]. This is an axisymmetric problem, in which vortex lines are circular with a common symmetry axis (taken as  $z$ -axis) and the vorticity has only the azimuthal component in the cylindrical coordinate system  $(z, R, \phi)$ , *i.e.*  $\boldsymbol{\omega} = (0, 0, \omega(z, R))$ . Using the spherical coordinates  $\boldsymbol{x} = (r, \theta, \phi)$ , the observation point is represented by the cartesian coordinates  $\boldsymbol{x} = (x, y, z)$ , where  $x = r \sin \theta \cos \phi$ ,  $y = r \sin \theta \sin \phi$ , and  $z = r \cos \theta$ . Then, the tensors  $Q_{ij}$  of (49) are found to be diagonal:

$$Q_{zz} = -2Q_{xx} = -2Q_{yy} := (1/6)Q(t), \quad Q_{ij} = 0 \quad (i \neq j),$$

where

$$Q(t) := \iint zR^2 \omega(z, R, t) dz dR. \quad (52)$$

Thus, the far field acoustic pressure (50) generated by the head-on collision of two vortex rings is reduced to

$$p(r, \theta, t) = \frac{\rho_0}{4c^2} \frac{1}{r} (\cos^2 \theta - \frac{1}{3}) Q'''(t - r/c), \quad (53)$$

where  $r, \theta$  are the coordinates of the observation point. The azimuthal component of the vorticity  $\omega(z, R, t)$  is governed by the vorticity equation (12), and determines the time evolution of the function  $Q(t)$ . Thus, once the vorticity  $\omega(z, R, t)$  is found by solving the vorticity equation, then we obtain the wave field generated by the vortex motion, characterized with the quadrupolar field by the factor  $(\cos^2 \theta - 1/3)$ .

This formulation can be applied to a discrete set of  $N$  circular vortex rings whose common axis coincides with the  $z$  axis. The factor  $\omega dz dR$  in the integrand of (52) stands for the strength ( $d\Gamma$ , say) of an elemental vortex ring at  $(Z, R)$ . The function  $Q(t)$  for  $N$  vortex rings of radius  $R_i$  located at the axial position  $z = Z_i$  ( $i = 1, \dots, N$ ) can be written as

$$Q(t) = \sum_{i=1}^N Z_i R_i^2 \Gamma_i, \quad (54)$$

where  $\Gamma_i$  is the strength of the  $i$ -th vortex.

Head-on collision of two identical vortex rings ( $i = 1, 2$ ) with opposite circulations is represented by  $N = 2$  (Fig. 1), and we may set  $R_1 = R_2 \equiv R(t)$ ,  $Z_1 = -Z_2 \equiv Z(t)$  ( $>0$ ) and  $-\Gamma_1 = \Gamma_2 \equiv \Gamma(>0)$ , where the mid-plane of collision is at  $z = 0$ . Thus, we have

$$Q(t) = -2\Gamma R^2(t) Z(t). \quad (55)$$

The orbits ( $\pm Z(t)$ ,  $R(t)$ ) of the vortices in the inviscid fluid can be calculated by solving a set of ordinary differential equation, which was carried out in [31]. Those data can be used to obtain the time factor  $Q''''_{\text{inv}}(t)$  of the pressure field (53). Thus we obtain the temporal profile of the vortex sound. An example of instantaneous spatial directivity is shown in Fig. 2, where the solid quadrupolar curve corresponds to the time of the first positive peak of the observed  $p_q$  of Fig. 3.

#### 4. VORTEX SOUND IN A REAL VISCOUS FLUID

Experimental detections of vortex sound in the air were made for head-on collision (Kambe & Minota [32]) and for oblique collision of two vortex rings (Kambe *et al.* [34]). Observed waves were in good agreement with theoretical predictions. In particular, a third-order component is found to be significant in the case of oblique collision. The *real* means that the fluid is compressible and viscous, and hence the kinetic energy  $K$  is not invariant. Reconnection of vortex lines occurs in the oblique collision due to the viscosity effect, which was studied by [1], [22], [34] and [52].

##### 4.1. General problem

The general higher order expansion formula (33) of the velocity potential (for the inner field) in §3.1 can be applied to obtain the wave pressure in the outer field emitted by general three-dimensional vortex motions in a viscous fluid. Note that the flow is irrotational in the far field so that the pressure is given by the relation,  $p = -\rho_0 \partial_t \Phi$ . Thus, for an oblique collision of two vortex rings, the acoustic pressure at  $r = |x|$  ( $= x$ ) in the far field is given by

$$\begin{aligned} p(\mathbf{x}, t) = & \frac{5 - 3\gamma}{12} \frac{\rho_0}{\pi c^2} \frac{1}{r} K^{(2)}(t_r) + \frac{\rho_0}{c} \frac{x_i}{r^2} Q_i^{(2)}(t_r) - \frac{\rho_0}{c^2} \frac{x_i x_j}{r^3} Q_{ij}^{(3)}(t_r) \\ & + \frac{\rho_0}{c^3} \frac{x_i x_j x_k}{r^4} Q_{ijk}^{(4)}(t_r) + \dots, \end{aligned} \quad (56)$$

[34], where  $p$  is used instead of  $p_F$ , the functions  $Q_i(t)$ ,  $Q_{ij}(t)$  and  $Q_{ijk}(t)$  are defined by (34) and (35),  $t_r \equiv t - r/c$  (retarded time), and

$$K(t) = \frac{1}{2} \int v^2 d^3 \mathbf{y}, \quad (57)$$

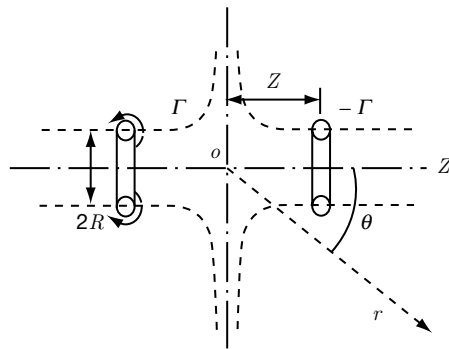


**Figure 1:** Head-on collision of two vortex rings (definition).

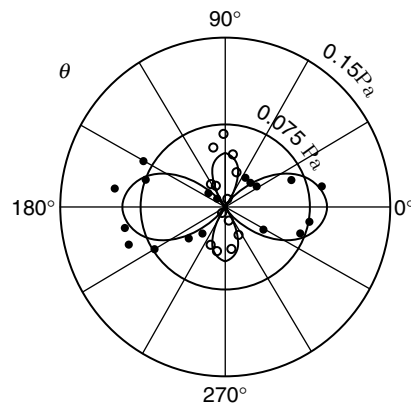


**Figure 2:** Quadrupolar curve ( $\cos^2 \theta - 1/3$ ) by the solid line. Observed pressures by  $\circ$  (positive) and  $\bullet$  (negative). [45]

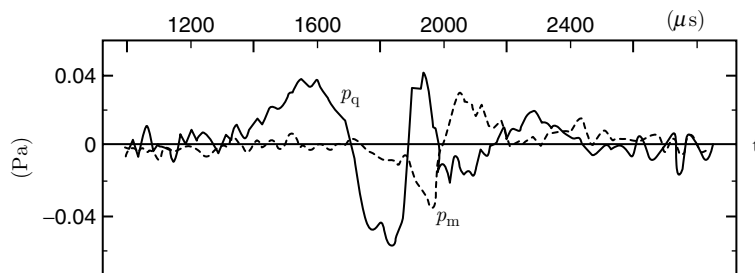


**Figure 3:** Observed amplitudes  $p_m(t)$  and  $p_q(t)$ . [45]

$\gamma$  being the ratio of specific heats ( $\gamma = 7/5$  of the air leads to  $(5 - 3\gamma)/12 = 1/15$ ). The superscript ( $n$ ) denotes the  $n$ -th time derivative, *e.g.*  $Q_{ij}^{(3)}(t) = Q_{ij}'''(t)$ . This formula was derived from the expansion (33). Its first term yields the first monopole term of (56) which is non-vanishing owing to dissipation of the (total) kinetic energy  $K$ , while the second term of (33) yields a dipole term which vanishes here because the flow impulse  $P_i$  is conserved in the absence of external forces or solid bodies. The sound emission in the presence of solid bodies is considered in the next section.

For the collision of two vortices in the air [45], the monopole term was detected although the amplitude was very small. In the axisymmetric case of head-on collision of two vortex rings, the fourth term  $Q_{ijk}^{(4)}$  vanishes by the symmetry. However, in the oblique collision, those terms are significant, and in fact the term  $Q_{ijk}^{(4)}$  was observed in the experiment [34].

## 4.2. Head-on collision of two vortex rings

### 4.2.1. Experiment

The head-on collision of two vortex rings studied by [32] is an axisymmetric problem. Then, the formula (56) reduces to

$$p(\mathbf{x}, t) = \frac{1}{15} \frac{\rho_0}{\pi c^2 r} K^{(2)}(t_r) + \frac{\rho_0}{4c^2 r} (\cos^2 \theta - \frac{1}{3}) Q'''(t - r/c), \quad (58)$$

where (53) is substituted, and fourth and higher order terms are neglected.

The experimental detection was made at a fixed radial distance of  $r_* = 630$  mm from the center of collision of two vortex rings with the initial radius  $R(0) = 4.7$  mm and initial velocity  $U = |\dot{Z}(0)| = 34$  m/s. Reynolds number defined by  $Re = UR(0)/\nu$  was about  $1.1 \times 10^4$ . After laborious analysis of the observed data, average profiles of detected acoustic pressure were determined, and finally reduced to the following form:

$$p(r_*, t) = p_m(t) + p_q(t)(1 - 3\cos^2 \theta), \quad (59)$$

[45], where  $p_m(t)$  and  $p_q(t)$  are shown in Fig. 3 as functions of the time  $t$ . This form is consistent with (58). The first term  $p_m(t)$  is proportional to  $K''(t)$ . Therefore, the term  $p_m(t)$  signifies how the total kinetic energy changed during the collision. The symbols  $\circ$  and  $\bullet$  in the diagram of Fig. 2 represent the detected pressures at the corresponding angle  $\theta$  at the time of the first positive peak of the observed  $p_q$ .

The factor  $p_q(t)$  corresponds to  $Q_{inv}'''(t)$  given at the end of §3.5. Comparing the profiles  $Q_{inv}'''(t)$  (inviscid) with  $p_q(t)$  (observation) in Fig. 4, it is found that the first half of both profiles corresponds very well to each other, while in the second half of the colliding process, both differ significantly. This difference may be interpreted as follows. In the final stage of the collision of two vortices, the viscosity plays a significant role in the interaction since the cores of each vortex come into contact (the profiles  $Q_{dns}'''(t)$  will be explained just below). Compressibility effect in the collision of

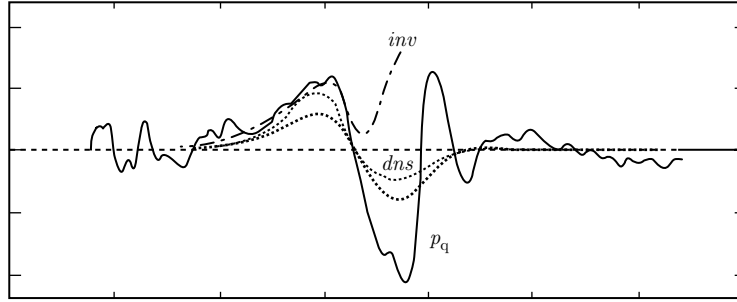


**Figure 4:** Comparison of three profiles:  $p_q(t)$  (solid curve),  $Q_{inv}'''(t)$  (chain-dotted), and  $Q_{dns}'''(t)$  (two broken curves for two different  $Re$ -values).

two vortices is investigated by [49]. Note that there is a difference in the details between the observed curves of  $p_q(t)$  of Fig. 3 and Fig. 4, because those were obtained with different experimental tests. The former data is taken from Data II ( $Re \approx 1.1 \times 10^4$ ), while the latter is from Data III ( $Re \approx 1.5 \times 10^4$ ) of [45].

#### 4.2.2. DNS

A direct numerical simulation (DNS) was carried out by taking advantage of advanced performance of computer resources by [23] to obtain the time factor  $Q'''(t)$  (shown by  $Q_{dns}'''(t)$  in Fig. 4) for the vortex collision in a viscous fluid (Fig. 16 (a) of [23]). Navier-Stokes equation was solved numerically for a compressible viscous fluid by a finite difference method, with spatial derivatives of a sixth-order compact Padé scheme proposed by Lele [40]. Time integration was the Runge-Kutta scheme. It is concluded there that the vortex-sound theory predicts the details of waves in the far field very well. The agreement with the experimental observations is qualitative because the DNS was performed at a Reynolds number lower ( $Re = 500$  (weaker), 2000 (stronger)) than that ( $Re \approx 1.5 \times 10^4$ ) of the experiment [45] by an order of magnitude.

The DNS presents some evidence of existence of monopole term  $p_m$  in Fig. 16 (b) of [23], although its amplitude is much smaller because of the lower Reynolds numbers of DNS. Another case of DNS of *oblique collision* of two vortex rings to be described in §4.3.3 also presents some evidence of monopole term  $p_m$  in Fig. 13 (a) of [52]. Viscosity effect is also considered in [50]. Since the monopole term depends on the second time derivative of the total kinetic energy, it is considered to be non-negligible even if Reynolds number increases because its rate of change becomes significant in those cases although the viscosity becomes small.

### 4.3. Oblique collision of two vortex rings

#### 4.3.1. Formulations

A mathematical formulation is presented for general higher-order expansions of the wave form by Kambe *et al.* [34], which is already described in §3. It is expected in this oblique collision that there is a process of reconnection of vortex lines at the time of

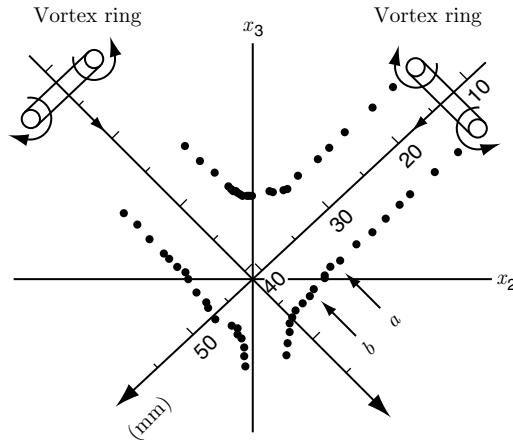


**Figure 5:** Observed trajectories of vortex cores in  $(x_2, x_3)$  plane. [34]

collision. This is investigated in particular by a new approach of vorticity-potential method by Ishii *et al.* [22] to solve numerically the three-dimensional viscous vorticity equation.

#### 4.3.2. Experiment

In addition to the mathematical formulation described above, experimental investigation was also made by [34] for acoustic waves generated by oblique collision of two vortex rings. The acoustic pressure of the form (56) can be rewritten by using the spherical polar coordinates  $(r, \theta, \phi)$ . The experiment was arranged such that the centers of two vortex rings move along the paths intersecting at right angles at the origin and collide with one another (Fig. 5). The bisecting straight line between the two paths of the vortex centers is taken as the polar axis  $\theta = 0$ , also taken as the  $x_3$  axis. The  $(x_1, x_2)$ -plane is defined by  $\theta = \pi/2$ , and the plane  $\phi = 0$  is taken along the positive  $x_1$  axis, and the trajectories of the vortex-centers are included in the  $(x_2, x_3)$  plane. Observed trajectories of the vortex cores in the  $(x_2, x_3)$ -plane are shown by dots in Fig. 5.

Symmetry consideration leads to the following expression for the far-field acoustic pressure, from (56), at a fixed radial distance  $r_*$  from the origin:

$$\begin{aligned}
 p(\theta, \phi, t) \Big|_{r_*} = & A_0(t) + A_1(t)P_2^0(\cos \theta) + A_2(t)P_2^2(\cos \theta) \cos 2\phi \\
 & + B_1(t)P_3^0(\cos \theta) + B_2(t)P_3^2(\cos \theta) \cos 2\phi,
 \end{aligned} \tag{60}$$

where  $P_n^m(z)$  are the Legendre polynomials with respect to  $z$  (shown up to  $n = 3$ ), and higher order terms are omitted since observed mode amplitudes were found to be insignificant. The first two terms corresponds to (59). There are five amplitude functions,

$$A_0(t), A_1(t), A_2(t), B_1(t), B_2(t).$$

These must be determined from the observed signals. Figure 6 shows an asymmetric emission at an instant, which is the distribution in the  $(x_1, x_3)$ -plane ( $\phi = 0$  and  $\pi$ ), obtained from (60) with using the observed coefficients at  $t = 5.12$  ms of Fig. 7 of [34].

### 4.3.3. DNS

Direct numerical simulation (DNS) was carried out by [52, 53] for oblique collision of two vortex rings with updated performance of computer resources. The five mode amplitudes were calculated from the DNS data and compared with those of experimental signals of [34]. Both results showed good qualitative agreement, although Reynolds numbers and Mach numbers were different between them. The DNS's were carried out for another initial conditions of oblique angles (other than at right angles).

A remarkable feature of the oblique collision is that there is reconnection of vortex lines at the time of collision. The DNS study has an advantage in that a part of the wave profile can be identified with the process of reconnection of vortex lines. In addition, DNS enables to relate each wave pulse with each part of the vortex motion as a source by using the theoretical formulation presented in the previous sections.

## 5. SOUND EMISSION BY VORTEX-BODY INTERACTION

### 5.1. Dipolar emission

When there is a solid body in the vicinity of vortex motion, the wave field changes its character and shows an emission of dipolar type rather than the quadrupolar emission considered so far in free space. The boundary condition to be satisfied on the body surface causes more powerful emission of dipole nature. Time-dependent pressure over the body surface results in time-dependent net force acting on the body. Conversely the fluctuating force, multiplied by a minus sign, is equivalent to the rate of change of the total fluid momentum.

In the presence of a solid body of size  $O(l)$  near the vortex motion, the Green's function is given approximately by

$$G_B(\mathbf{x}, \mathbf{y}) = \frac{1}{4\pi |\mathbf{x} - \mathbf{Y}(\mathbf{y})|}, \quad (61)$$

$$\mathbf{Y}(\mathbf{y}) = \mathbf{y} + \Phi(\mathbf{y}), \quad (62)$$

according to the theory of vortex sound [17, 26, 56]. (Green's function satisfying the wave equation (rather than (39)) is considered in Chap. 3 of Howe [20] in an acoustically compact case.) The expression (61) is valid when  $x$  is far from the body, *i.e.*  $|\mathbf{x}| \gg l$ , where the coordinate origin is taken within the body. The vector function  $Y_i(\mathbf{x})$  denotes a velocity potential (*i.e.*  $\nabla^2 Y_i = 0$ ) of a hypothetical flow around the

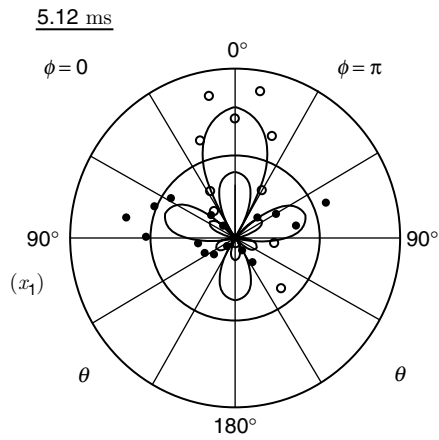


**Figure 6:** Asymmetric emission of the oblique collision at an instant. Observed pressures by  $\circ$  (positive) and  $\bullet$  (negative). Solid curve is from (60) (at  $t = 5.21$  ms of Fig. 7 of [34]).

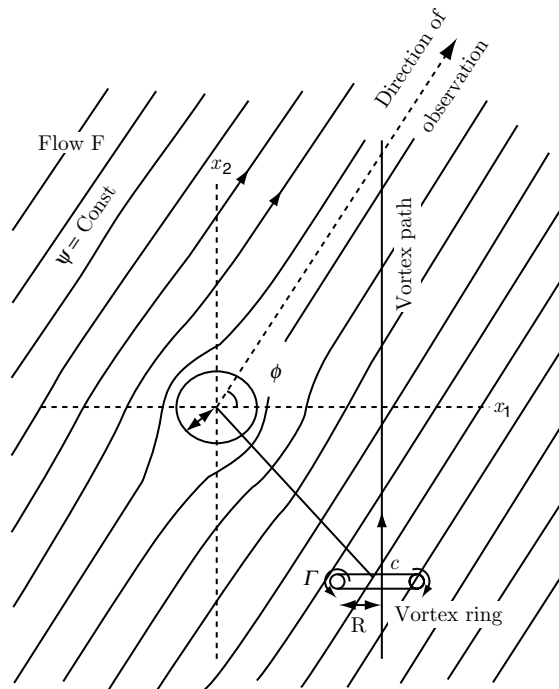


**Figure 7:** Schematic diagram: Vortex path and streamlines ( $\Psi = \text{const}$ ) of a hypothetical potential flow (to the observation direction) around the cylinder.

body with a unit velocity to the  $y_i$  direction at infinity ( $i = 1, 2, 3$ ). The first term  $y_i$  represents the uniform flow of a unit velocity and the vector function  $\Phi_i(\mathbf{y})$  represents a correction due to the presence of a body which imposes the boundary condition of vanishing normal velocity:  $\mathbf{n} \cdot \nabla \mathbf{y} Y_i = 0$  for  $\mathbf{y}$  on the body surface S. When there is no solid body, we have  $\Phi_i = 0$ . Then the function (61) reduces to (45) for the free space. The function  $G_B(\mathbf{x} - \mathbf{y})$  satisfies the following condition on the body surface S:

$$\mathbf{n} \cdot \nabla \mathbf{y} G_B(\mathbf{x} - \mathbf{y}) = 0, \quad \text{for } \mathbf{y} \text{ on S.} \quad (63)$$

This is verified by differentiating (61) with respect to  $y_i$ . In fact, we have

$$\nabla \mathbf{y} G_B(\mathbf{x}, \mathbf{y}) = \frac{(x_i - Y_i) \nabla \mathbf{y} Y_i}{4\pi |\mathbf{x} - \mathbf{Y}(\mathbf{y})|^3}. \quad (64)$$

Hence, the boundary condition  $\mathbf{n} \cdot \nabla \mathbf{y} Y_i = 0$  (on S) implies (63). It is readily seen that the function  $G_B$  tends to  $1/[4\pi|\mathbf{x} - \mathbf{y}|]$  as  $x/l$  and  $y/l \rightarrow \infty$ , since we have  $|\Phi(\mathbf{y})| = O(y^{-2})$  for a body of size  $O(l)$ . See the last part of §3.1 for asymptotic property of velocity  $v_i$ .

For  $|\mathbf{x}| \gg |\mathbf{y}|$  in (61), we develop it in a form similar to (32), but using  $Y_i$  in place of  $y_i$ , and apply the operator  $\nabla^2 \mathbf{y}$ . Then, the first two terms disappear (since  $\nabla^2 Y_i = 0$ ), and the third term is

$$\nabla^2 \mathbf{y} G_B = \frac{1}{8\pi} \nabla^2 (Y_i Y_j) \frac{\partial^2}{\partial x_i \partial x_j} \frac{1}{x} = O(x^{-3}).$$

Therefore the function  $G_B$  satisfies the equation  $\nabla^2 G_B = 0$  within an error of  $O(x^{-3})$ . Note that the term  $\nabla \mathbf{y} G_B$  to be used in the following is a lower-order term of  $O(x^{-2})$  (see below). Thus up to that order,  $G_B$  has the correct behavior (as a function satisfying (39)). This permits us to use (61) as the Green's function in the present context. Using an asymptotic expansion of the form (32) as  $x \rightarrow \infty$ , the expression (64) is written as

$$\nabla \mathbf{y} G_B = \frac{x_i}{4\pi x^3} \nabla \mathbf{y} Y_i + O(x^{-3}). \quad (65)$$

The velocity field of the potential flow given by  $\nabla \mathbf{y} Y_i$  is solenoidal in the  $\mathbf{y}$ -space. This permits introduction of a vector potential  $\Psi_i(\mathbf{y})$  (a vector for each  $i = 1, 2, 3$ ) by the relation,

$$\nabla \mathbf{y} Y_i = \nabla \mathbf{y} \times \Psi_i, \quad \text{div } \Psi_i = 0 \quad (i = 1, 2, 3). \quad (66)$$

Each component of  $\Psi_i$  is harmonic since  $0 \equiv \nabla \times (\nabla \times \Psi) = -\nabla^2 \Psi_i$ . One may choose that  $\Psi_i = 0$  on S without violating (66). Using (65) and (66) in (43), one obtains

$$p_1(\mathbf{x}, t) = -\frac{\rho_0}{4\pi} \frac{x_i}{x^3} \int \mathbf{L} \cdot (\nabla \mathbf{y} \times \Psi_i) d^3 \mathbf{y} + O(x^{-3}). \quad (67)$$

Integrating by parts and using (12), one finds

$$p_1(\mathbf{x}, t) = -\frac{\rho_0}{4\pi} \dot{\Pi}_i \frac{\partial}{\partial x_i} \frac{1}{x} + O(x^{-3}), \quad (68)$$

$$\dot{\Pi}_i(t) = \frac{d}{dt} \Pi_i(t), \quad \Pi_i(t) \equiv \int \boldsymbol{\omega}(\mathbf{y}, t) \cdot \Psi_i(\mathbf{y}) d^3 \mathbf{y}. \quad (69)$$

Thus the inner pressure is of the form of a dipole potential in the leading order.

Corresponding outer pressure (see §3.3.2 and 3.3.3) is given by

$$p_o(\mathbf{x}, t) = -\frac{\rho_0}{4\pi} \frac{\partial}{\partial x_i} \frac{\dot{\Pi}_i(t - x/c)}{x}. \quad (70)$$

In the far field as  $\hat{x} = x/\lambda \rightarrow \infty$ , this reduces to

$$p_f(\mathbf{x}, t) \frac{\rho_0}{4\pi c} \ddot{\Pi}_i(t - x/c) \frac{x_i}{x^2}. \quad (71)$$

Operating  $\partial_i$  to the factor  $1/x$  gives a higher order term of  $O(1/x^2)$ , which is neglected. This represents a dipolar emission by the vortex-body interaction.

From (71), scaling law of the dipolar wave can be deduced as carried out in §3.4. The function  $\Pi_i$  is normalized by  $ul^3$ , since  $\boldsymbol{\omega} \sim u/l$  and  $|\Psi_i| \sim l$ . Hence  $|\ddot{\Pi}_i|$  by  $ul^3/\tau^2 = u^3l$ . Thus the scaling law of pressure of the dipole sound, denoted by  $p_D$ , is given by

$$p_D \sim \frac{\rho_0}{c} \frac{1}{r} u^3 l = \frac{\rho_0 u^3}{c} \frac{1}{r}. \quad (72)$$

The sound intensity is  $I_D \sim (\rho_0 u^6/c^3)(l/r)^2 \propto u^6$  (where  $r = |\mathbf{x}|$ ).

## 5.2. Emission from a loop vortex

The dipole-emission law (71) has an interesting property explained as follows. Suppose that there exists a vortex filament (of strength  $\Gamma$ ) forming a closed loop, of which the centerline is denoted by a closed curve  $C_v$ . Writing a line element of  $C_v$  as  $d\mathbf{s}$  and representing the vortex filament as  $\boldsymbol{\omega} = \Gamma d\mathbf{s}$ , the integral  $\Pi_i(t)$  of (69) is rewritten as

$$\Pi_i(t) = \Gamma \int_{C_v} \Psi_i(\mathbf{s}) \cdot d\mathbf{s} = \Gamma \int_{S_v} (\nabla \mathbf{y} \times \Psi_i(\mathbf{y})) \cdot \mathbf{n} \, dS(\mathbf{y}). \quad (73)$$

where  $S_v$  is an open surface with the circumference bounded by the closed curve  $C_v$ , and  $\nabla \times \Psi_i$  represents the velocity of a hypothetical potential flow (with a unit velocity in the  $y_i$  direction) around the body. It is found that the second expression of  $\Pi_i$  represents the volume flux  $J_i$  of the hypothetical flow through the loop  $C_v$  multiplied by  $\Gamma$ :

$$\Pi_i(t) = \Gamma J_i(t), \quad J_i(t) = \int_{S_v} (\nabla \times \Psi_i) \cdot \mathbf{n} \, dS. \quad (74)$$

Although the potential flow  $\nabla \times \Psi_i$  is steady, the flux  $J_i$  is time-dependent because the vortex position (represented by the curve  $C_v$ ) changes.

Thus, the following law is found. When a vortex ring (not necessarily circular) moves near a solid body, the flux  $J_i$  through  $C_v$  changes with the time  $t$ , which causes sound emission according to (71):

$$p_{\text{F}}(\mathbf{x}, t) = \frac{\rho_0 \Gamma}{4\pi c} \ddot{J}_i \left( t - \frac{x}{c} \right) \frac{x_i}{r^2}. \quad (75)$$

This phenomenon is *analogous* to the Faraday's law in the electromagnetism, and may be called as *acoustic Faraday's law*. (The present case of vortex sound is valid in an asymptotic sense. However, the Faraday's law in the electromagnetism is valid rigorously.) Note that  $(x_i/r)J_i$  denotes the volume flux of a hypothetical flow (through  $C_v$ ) heading for the observation direction  $x_i/r$ . Figure 7 is a diagrammatic interpretation of the acoustic Faraday's law in the near-field of source region. Experimental study was made for solid bodies such as a circular cylinder [46] or a sphere [47]. The next subsection describes the former study.

### 5.3. Vortex ring passing nearby a circular cylinder

#### 5.3.1. Directivity of wave emission

Suppose that a circular vortex ring of strength  $\Gamma$  and radius  $R$  passes by a circular cylinder of radius  $a_c$  of infinite length. The  $x_3$  axis is taken along the cylinder axis (Fig. 7). If the vortex position is sufficiently far from the cylinder, the vortex path may be regarded as rectilinear. It is assumed that the vortex keeps its circular form, and the ring center moves in the plane  $(x_1, x_2)$  perpendicular to the  $x_3$  axis. This means that the normal  $\mathbf{n}$  to the ring-plane is orthogonal to the  $x_3$ . Then, the expression (71) reduces to

$$p(\mathbf{x}, t + \frac{r}{c}) = \frac{\rho_0}{4\pi c} \Gamma \frac{\sin \theta}{r} [\ddot{J}_1(t) \cos \phi + \ddot{J}_2(t) \sin \phi] \quad (76)$$

$$= \frac{\rho_0}{4\pi c} \Gamma \frac{\sin \theta}{r} \ddot{J}(t) \cos(\phi - \Theta(t)), \quad (77)$$

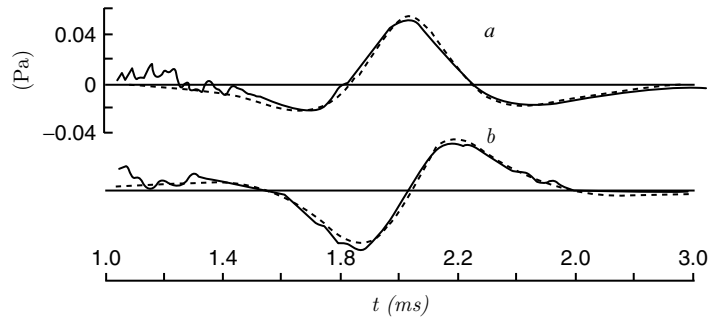


**Figure 8:** Comparison in absolute values between observed (solid) and predicted (two broken curves by two model vortices) coefficients  $a(t)$  and  $b(t)$ . [46]

(Minota & Kambe [46]),<sup>2</sup> where  $\ddot{J} = (\ddot{J}_1^2 + \ddot{J}_2^2)^{1/2}$  and  $\tan \Theta = \ddot{J}_2 / \ddot{J}_1$ , and  $J_3$  is zero since  $\Psi_3$  denotes a uniform flow parallel to the  $x_3$  axis perpendicular to  $\mathbf{n}$ . The angle  $\phi$  denotes the azimuthal angle of the projection  $(x_1, x_2, 0)$  of the vector  $\mathbf{x}$ , measured from the  $x_1$  axis. The angle  $\theta$  is the polar angle of  $\mathbf{x}$  from the  $x_3$  axis.

The directivity of the acoustic emission (77) is of dipole character, where the direction of dipole axis is given by the angle  $\Theta(t)$ . Note that the wave pressure (77) vanishes toward the cylinder axis  $\theta = 0$  and  $\pi$ .

### 5.3.2. Experimental detection

Experimental investigation of the acoustic waves generated by a vortex passing by a circular cylinder was also made by [46]. Average observed pressure in the plane  $\theta = 90^\circ$  is expanded into the Fourier series with respect to  $\phi$ . It is found that main component is given by the form,

$$p_{\text{obs}} = -a(t)\sin \phi + b(t)\cos \phi \tag{78}$$

in accordance with (76). The solid curves in Fig. 8 are observed profiles, while the broken curves are the profiles according to the theory described in §5.1 ~ 5.3. Agreement in absolute values between the observed and predicted profiles is excellent.

## 6. SOUND GENERATION BY A CYLINDER IN UNIFORM FLOW

Viscous flow around a circular cylinder is one of the standard problems in fluid mechanics. At a certain range of values of Reynolds number, vortices of opposite senses of rotation are shed alternately from the cylinder surface periodically. This causes radiation of sound waves of dipole character. This subject is called sometimes as a problem of *aeolian tones*. Strouhal (1878) [59] found experimentally that the frequency  $f$  of sound radiated from a cylinder of radius  $a$  in a uniform flow of velocity  $U$  is scaled

<sup>2</sup>The angle notations of  $\theta$  and  $\phi$  are interchanged with those of [46].

as  $U/a$ , so that the non-dimensional combination  $fa/U$  takes almost-constant value, now known as the Strouhal number.

### 6.1. Curle's formula

The wave density  $\rho(\mathbf{x}, t)$  is governed by Eq. (6), which is transformed to the following integral form in the presence of a solid body B with surrounding surface  $\partial B$  (Curle [11]):

$$\rho'(\mathbf{x}, t) = \frac{1}{4\pi c^2} \frac{\partial^2}{\partial x_i \partial x_j} \int_V \frac{T_{ij}(\mathbf{y}, t_r)}{|\mathbf{x} - \mathbf{y}|} d^3\mathbf{y} - \frac{1}{4\pi c^2} \frac{\partial}{\partial x_i} \int_{\partial B_3} \frac{n_j p_{ij}(\mathbf{y}, t_r)}{|\mathbf{x} - \mathbf{y}|} dS(\mathbf{y}), \quad (79)$$

where  $t_r = t - |\mathbf{x} - \mathbf{y}|/c$ ,  $T_{ij}$  is defined by (7),  $p_{ij} = p\delta_{ij} - \sigma_{ij}$  is the stress tensor and  $\sigma_{ij}$  the viscous stress, and  $V$  denotes the whole flow domain around a three-dimensional body  $B_3$  with  $n_i$  being unit outward normal from  $\partial B_3$ . This formula tells us that the sound field is represented by the sum of that generated by a volume distribution of quadrupoles  $T_{ij}$  and that by a surface distribution of dipoles  $p_{ij}$ .

Two-dimensional case (2D) was given (with  $r = |\mathbf{x}|$ ) by Hatakeyama & Inoue [16] as

$$\begin{aligned} c^2 \rho'(\mathbf{x}, t) = & \frac{x_i x_j}{2^{3/2} \pi c^{3/2} r^{5/2}} \int_{-\infty}^{t-r/c} \frac{dt'}{\sqrt{\tau - t'}} \frac{\partial^2}{\partial t'^2} \int_V T_{ij}(\mathbf{y}, t') d^3\mathbf{y} \\ & + \frac{x_i}{2^{3/2} \pi c^{1/2} r^{3/2}} \int_{-\infty}^{t-r/c} \frac{dt'}{\sqrt{\tau - t'}} \frac{\partial}{\partial t'} \int_{\partial B_2} f_i(\mathbf{y}, t') dS(\mathbf{y}), \end{aligned} \quad (80)$$

for a two-dimensional body  $B_2$  (formulae without the second term were given by Ffowcs-Williams [14] or Howe [19]).

### 6.2. DNS

Two-dimensional problem of direct numerical simulation of sound generation by a circular cylinder of diameter  $d$  placed in a uniform flow was carried out by [24]. Navier-Stokes equation was solved numerically for a compressible viscous fluid by a finite difference method, with spatial derivatives of a sixth-order compact Padé scheme proposed by Lele [40]. Time integration was the fourth-order Runge-Kutta scheme. The computational domain is divided into three regions of different grid spacings: a near field, an intermediate wave region, and a far field where pressure waves become sufficiently small and non-reflecting boundary condition can be applied.

Initial flow field is given in the  $(x, y)$ -plane by imposing a potential flow with a uniform flow of velocity  $U$  to the positive  $x$ -direction, except an artificial boundary layer on the cylinder surface. At a time of initial development, a small perturbation was added in order to force earlier transition to vortex streets. Figure 9 shows comparison of pressure distributions obtained at a fully-developed state by DNS (left) and Curle's integral solution (right). The data were obtained with Mach number of uniform flow

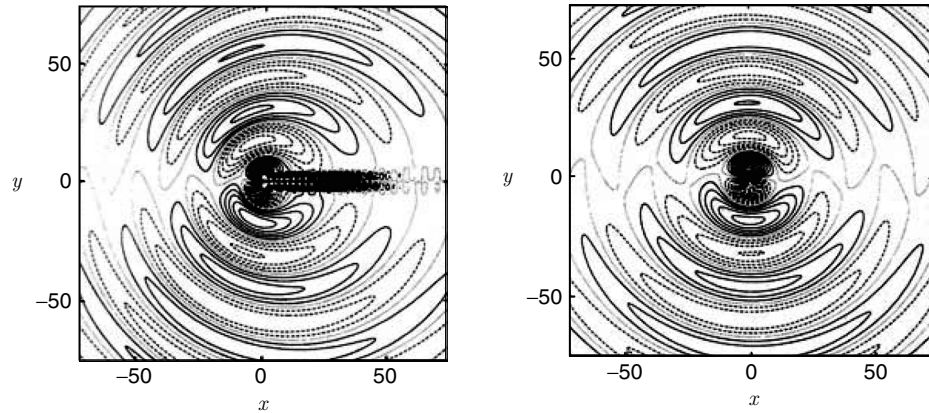


**Figure 9:** Pressure distributions of DNS (left) and Curle's dipole component (right), the center of cylinder (its radius 0.5) being at the origin (0, 0). Inoue and Hatakeyama [24].

$M = U/c = 0.2$  and Reynolds number  $Re = Ud/\nu = 150$  at a normalized time  $Ut/d = 1000$  (with the time step  $\Delta t = 0.002$ ).

The left-hand diagram of Fig. 9 shows the DNS result of fluctuation pressure  $\tilde{\Delta p}(x, y, t)$  defined by  $\Delta p - \overline{\Delta p}$ , where  $\overline{\Delta p}(x, y)$  is the mean pressure field. (Note:  $\overline{\Delta p}(x, y)$  is defined by the time average of  $\Delta p = p(x, y, t) - p_0$ , where  $p_0$  is the uniform pressure at infinity.) The right-hand diagram shows the wave pressure obtained by the second term (dipole component) of Curle's integral solution (80) with using the DNS data for the source term  $f_i(\mathbf{y}, t')$ . Evidently, it is seen that there is a difference between them. The contour patterns of DNS fluctuation  $\tilde{\Delta p}$  is inclined to upstream direction, while the Curle's solution is symmetric. This difference can be interpreted by the convection effect of the flow [16], *i.e.* the speed of wave propagation is given by  $c(\theta) = c - U \cos\theta$  where the angle  $\theta$  is measured from the negative  $x$  axis. Namely, the speed  $c(\theta)$  is smaller toward the upstream direction than that of the downstream. Thus, the convection effect is missing in the Curle's integral, and it is found that the main component of the sound wave is characterized by a dipolar wave influenced by the uniform stream.

## 7. SOUND EMISSION BY VORTEX-EDGE INTERACTION

Sound emission is enhanced, if a solid surface  $S$  immersed in a stream has a sharp edge. Noise generation by turbulent eddies in the vicinity of a sharp edge was studied by [6] and [13]. Here, we are interested in sound generation by a vortex ring moving near an edge of a flat plate [33]. Note that two-dimensional problem of acoustic emission from a vortex filament moving around a half-plane was investigated by [8, 18, 15, 51].

### 7.1. General formulation

Before considering a specific case, we first present general formulation. Suppose that we have the following equation with a wave source of the form  $\partial \hat{L}_i / \partial x_i$ :

$$(c^{-2} \partial_t^2 - \nabla^2) p = \frac{\partial}{\partial x_i} \hat{L}_i, \quad (81)$$

instead of (6), and that the equation for a Green's function  $G(\mathbf{x}, \mathbf{y}; t)$  is given by

$$(c^{-2} \partial_t^2 - \nabla_x^2) G(\mathbf{x}, \mathbf{y}; t) = \delta(\mathbf{x} - \mathbf{y}) \delta(t), \quad (82)$$

with the boundary condition:

$$\mathbf{n} \cdot \nabla_{\mathbf{x}} G(\mathbf{x}, \mathbf{y}; t) = 0, \quad \text{for } \mathbf{x} \in S, \quad (83)$$

where  $\mathbf{n} = (n_i)$  is a unit outward normal to  $S$ . Then, the solution of (81) can be given by

$$p(\mathbf{x}, t) = - \int d\tau \int \hat{\mathbf{L}}(\mathbf{y}, \tau) \cdot \nabla_{\mathbf{y}} G(\mathbf{x}, \mathbf{y}; t - \tau) d^3 \mathbf{y}. \quad (84)$$

This satisfies the condition:  $\mathbf{n} \cdot \nabla p(\mathbf{x}, t) = 0$  for  $\mathbf{x} \in S$  (flat-plate surface). (On the flat surface of the plate with a constant  $\mathbf{n}$ , we have  $-\mathbf{n} \cdot \nabla p(\mathbf{x}, t) = \rho(\partial_t(\mathbf{n} \cdot \mathbf{v}) + \mathbf{v} \cdot \nabla(\mathbf{n} \cdot \mathbf{v})) = 0$  from (10) since  $\mathbf{n} \cdot \mathbf{v} = 0$ .)

For a small vortex moving at low Mach numbers ( $M \ll 1$ ) in an inviscid fluid, Lighthill's equation (6) reduces to

$$(c^{-2} \partial_t^2 - \nabla^2) p = \rho_0 \frac{\partial}{\partial x_i} \frac{\partial}{\partial x_j} v_i v_j. \quad (85)$$

This can be rewritten in the form of (81), since we have

$$\rho_0 \frac{\partial}{\partial x_i} \frac{\partial}{\partial x_j} v_i v_j = \frac{\partial}{\partial x_i} \hat{L}_i \equiv \nabla \cdot \hat{\mathbf{L}}, \quad \frac{\hat{\mathbf{L}}}{\rho_0} \equiv (\mathbf{v} \cdot \nabla) \mathbf{v} = \boldsymbol{\omega} \times \mathbf{v} + \nabla(v^2/2), \quad (86)$$

where the flow is assumed to satisfy  $\nabla \cdot \mathbf{v} = 0$  (*i.e.* incompressible by  $M \ll 1$ ), and (11) is used. The wave pressure is given by (84) with (86).

According to Möring's transformation [51], a vector function  $\mathbf{G}(\mathbf{x}, \mathbf{y}; t - \tau)$  is introduced by the relation,  $\nabla_{\mathbf{y}} G = \nabla_{\mathbf{y}} \times \mathbf{G}$  under the condition  $\mathbf{n} \times \mathbf{G} = 0$  for  $\mathbf{y} \in S$ . Substituting this in (84), we have

$$p(\mathbf{x}, t) = - \int d\tau \int \hat{\mathbf{L}}(\mathbf{y}, \tau) \cdot \nabla_{\mathbf{y}} \times \mathbf{G} d^3\mathbf{y} = -\rho_0 \int d\tau \int \mathbf{G} \cdot \nabla_{\mathbf{y}} \times (\boldsymbol{\omega} \times \mathbf{v}) d^3\mathbf{y},$$

where the second equality is obtained by using (86) after integration by parts. Using the vorticity equation of (12), we obtain finally the following expression ( $\partial_t = \partial / \partial t$ ):

$$p(\mathbf{x}, t) = \rho_0 \partial_t \int d\tau \int \mathbf{G}(\mathbf{x}, \mathbf{y}; t - \tau) \cdot \boldsymbol{\omega}(\mathbf{y}, \tau) d^3\mathbf{y}. \quad (87)$$

## 7.2. Vortex ring moving near by a semi-infinite plate

When a vortex ring moves near by a sharp edge of a semi-infinite plate, the wave emission is quite different from that by a circular cylinder. The plate is assumed to lie in the half-plane ( $x_1, x_3$ ) with negative  $x_1$ , and the edge is expressed by

$$x_1 = 0, \quad x_2 = 0, \quad -\infty < x_3 < \infty.$$

In this frame of reference, the vector Green's function  $\mathbf{G}$  can be given by

$$\mathbf{G}(\mathbf{x}, \mathbf{y}; t) = (0, 0, F) \partial_t^{1/2} \delta(t_r), \quad t_r = t - \frac{x}{c}, \quad (88)$$

$$F(\mathbf{x}, \mathbf{y}_2) = \frac{1}{\sqrt{2\pi^3 c x^3}} \Phi(\mathbf{x}) \Psi(\mathbf{Y}), \quad x = |\mathbf{x}|, \quad \mathbf{Y} = (y_1, y_2) \quad (89)$$

$$\Phi = (x \sin \phi)^{1/2} \sin \frac{1}{2} \theta, \quad \Psi = Y^{1/2} \cos \frac{1}{2} \theta \quad (90)$$

[33]. See below for the fractional time derivative  $\partial_t^{1/2}$ . This accounts for non-local time effect by the non-compact edge plate. Substituting  $\mathbf{G}$  of (88) into (87), we obtain

$$p(\mathbf{x}, t + \frac{x}{c}) = \frac{\rho_0}{\sqrt{2\pi^3}} \frac{(\sin \phi)^{1/2} \sin \frac{1}{2} \theta}{\sqrt{c x}} \left( \frac{d}{dt} \right)^{3/2} \int \Psi(\mathbf{y}) \boldsymbol{\omega}_3(\mathbf{y}, t) d^3\mathbf{y}, \quad (91)$$

where  $\phi = \cos^{-1}(x_3/x)$ . The fractional derivative is defined by

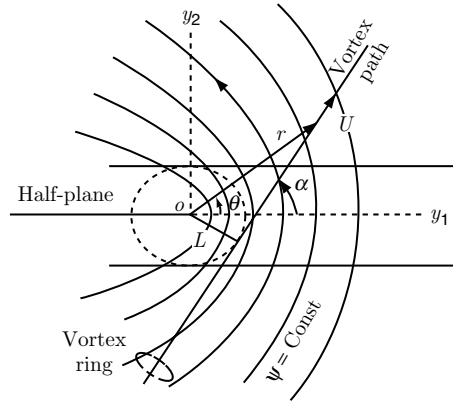


**Figure 10:** Schematic diagram: vortex path and streamlines of a hypothetical potential flow around the edge.

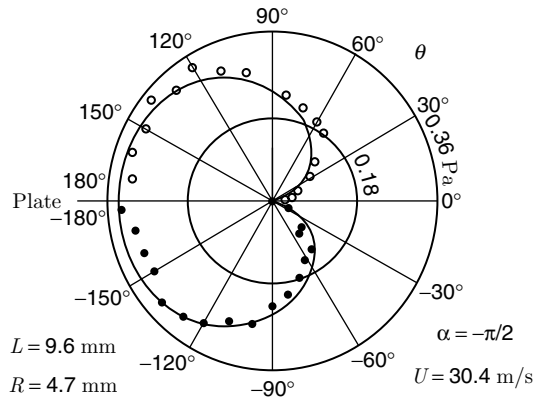


**Figure 11.** Observed pressures by  $\circ$  (positive) and  $\bullet$  (negative). Solid curve is  $f_{\text{obs}}(t_0) \sin \frac{1}{2} \theta$  at a fixed time  $t_0$ .

$$\left(\frac{d}{dt}\right)^{\frac{1}{2}} g(t) = \frac{1}{2\pi} \int_{-\infty}^{\infty} (-i\omega)^{\frac{1}{2}} \hat{g}(\omega) e^{-i\omega t} d\omega = \int_{-\infty}^t \hat{g}(s) \frac{ds}{[\pi(t-s)]}.$$

It is found that the acoustic pressure (91) is composed of the angular factor,

$$F(\theta, \phi) = (\sin \phi)^{\frac{1}{2}} \sin \frac{1}{2} \theta, \quad (\text{Cardioid})$$

and the time factor,

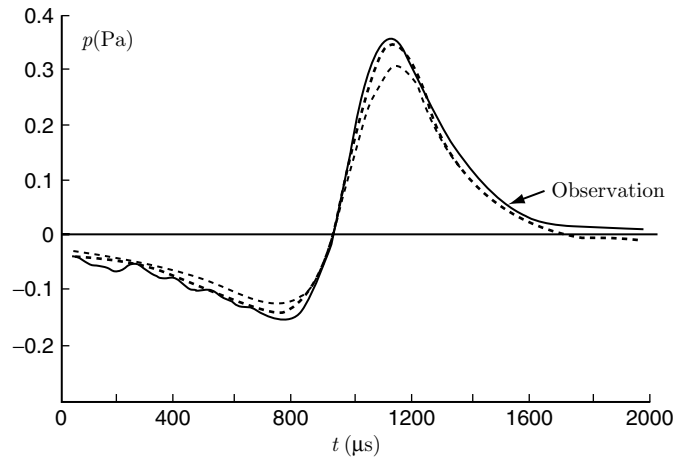


**Figure 12:** Comparison of temporal factor  $f(t)$  between observed (solid) and two calculated (broken-line) curves of the theory, for the acoustic pressure generated by a vortex passing the edge of a half-plane, detected at  $x = 634$  mm.

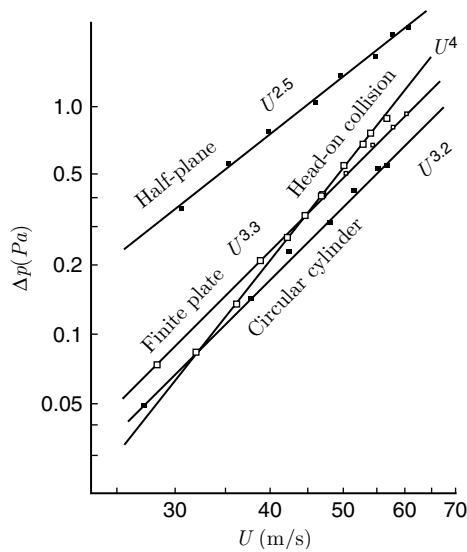


**Figure 13:** Observed power laws of  $\Delta p$  (Pa) vs.  $U$  (m/s). [26]. See Appendix B for the experimental data.

$$f(t) = \Gamma \left( \frac{d}{dt} \right)^{\frac{3}{2}} J(t), \quad J(t) = \int_S (\nabla \times \Psi) \cdot \mathbf{n} \, dS.$$

The function  $J(t)$  represents the volume flux  $J$  through the vortex ring of the hypothetical potential flow around the edge (Fig. 10). See [26, 33] for more details.

Note that the velocity  $\nabla \times \Psi$  of the hypothetical potential flow is scaled as  $L^{-1/2}$  ( $L$  being the closest distance to the edge), and that the time scale is  $\tau = L/u$ . The scaling law of the wave pressure is given by

$$p_E \sim \frac{\rho_0}{c^{1/2}} \frac{l^2}{L^2} \frac{1}{r} u^{5/2}. \quad (92)$$

The sound intensity is  $I_E \propto u^5/L^4$ .

### 7.3. Experiment

A laboratory experiment was carried out by Kambe *et al.* [33], in which a vortex ring of radius  $R = 4.7$  mm moved near the edge of a flat plate with the velocity  $U = 30.4$  m/s along a nearly straight path, the shortest distance being  $L = 9.6$  mm from the edge to the vortex center (Fig. 10). The observations showed the predicted cardioid distribution  $F(\theta, \pi/2)$  (Fig. 11).

Figure 12 shows a comparison in absolute values of the time factor  $f(t)$  between the observed curve  $f_{\text{obs}}(t)$  and the curves predicted by the theory given above, for a particular case of a vortex ring moving perpendicularly to the  $x_1$  axis from the positive to negative  $x_2$  in the  $(x_1, x_2)$ -plane and passing nearby the edge. Agreement between them is remarkable in absolute scales.

### 7.4. Note on the effect of vortex shedding<sup>3</sup>

Interaction of a vortex ring with the edge of an airfoil is considered in Howe [21], explaining how Kutta condition can be applied by modifying the Green's function. In the above mathematical analysis of vortex-edge interaction, shedding of vortices from the edge was disregarded, so that consideration is restricted only to the interaction of a vortex ring with an edge. Even though this is the case, agreement with the theoretical prediction was remarkable with respect to both directivity and magnitude in the experimental tests described above.

Present good agreement between them may be due to absence of mean flow in the above problem of vortex-edge interaction, where advection of separated eddies by the external flow may not be significant, *i.e.* rate of change of separated vortices may not be large enough to be detected as acoustic signal.

---

<sup>3</sup>This section is added in response to the comment of one of the referees.

## 8. VORTEX-SOUND IN SUPERFLUID

It is well-known that quantized vortex filaments and vortex rings are observed in super-fluid of Helium II [12]. The superfluid nature of weakly interacting atomic Bose-Einstein condensation (BEC) supports also quantized circulation [44]. Experimental observation of vortex rings in BEC is reported in [2]. A quantum mechanical model to describe quantized vortex lines is provided by a nonlinear Schrödinger equation, which is also called the Gross-Pitaevskii (GP) equation in the context of BEC. A condensate of  $N$  weakly interacting Bose particles of mass  $m$  is described by a wave function  $\Psi$  (called a complex order parameter), governed by the GP equation:

$$i\hbar\partial_t\Psi = -\frac{\hbar^2}{2m}\nabla^2\Psi + (V|\Psi|^2 - E)\Psi, \quad (93)$$

where  $V$  is the strength of the repulsive interaction between the bosons and  $E$  is the energy increase upon adding one boson. Expressing  $\Psi$  by  $A \exp(iS)$ , the imaginary and real part of (93) are transformed respectively to

$$\partial_t\rho + \operatorname{div}(\rho\mathbf{v}) = 0, \quad \partial_tv_i + (\mathbf{v}\cdot\nabla)v_i = -\partial_i h + \frac{1}{\rho}\partial_j\Sigma_{ij}, \quad (94)$$

( $\partial_i \equiv \partial/\partial x_i$ ), where the density  $\rho$ , velocity  $\mathbf{v}$  and stress tensor  $\Sigma_{ij}$  are defined by

$$\rho = mA^2, \quad \mathbf{v} = \frac{\hbar}{m}\nabla S, \quad \Sigma_{ij} = \frac{\hbar^2}{4m^2}(\partial_i\partial_j\rho - \frac{1}{\rho}\partial_i\rho\partial_j\rho).$$

The system of equations (94) is analogous to the equation (10) for an inviscid fluid since the term  $\rho^{-1}\partial_j\Sigma_{ij}$  can be transformed to a potential form  $\partial_i B$  (where  $B = (\hbar^2/2m^2)(\nabla^2 A/A)$ ), and the total energy is conserved [28, Ch.11]. The flow is irrotational since  $\mathbf{v} = (\hbar/m)\nabla S$ .

*Note:* The real part of GP equation corresponds to an integral  $\mathcal{R}$  of the equation of motion. In fact, using the relation  $\partial_j\Sigma_{ij}/\rho = \partial_i B$ , the second equation can be derived by operating  $\nabla$  to the real part  $\mathcal{R}$  of GP equation, given by  $\mathcal{R} \equiv (\hbar/m)\partial_t S + \frac{1}{2}v^2 - B - E/m + V_0 a^2/m (=0)$ , where  $\partial_i(\frac{1}{2}v^2) = (\mathbf{v}\cdot\nabla)v_i$  due to  $\boldsymbol{\omega} = \operatorname{curl}\mathbf{v} = 0$ . The GP equation supports quantized circulation, called quantum vortex, where the density vanishes at its center (a hollow vortex).

A computer experiment was carried out to simulate motion of a vortex in a magnetically trapped quasi two-dimensional BEC and its sound emission [57]. The vortex precesses around a center due to the inhomogeneous density of back-ground superfluid, and emits dipolar waves in a spiral pattern. The quasi-2D geometry ensures that the vortex line is effectively rectilinear.

A 2-dimensional homogeneous superfluid is equivalent to (2+1)-dimensional electrodynamics, where vortices play the role of charges and sound corresponds to electromagnetic radiation [37].<sup>4</sup> By analogy to the Larmor radiation for an accelerating charge, it is found that the vortex energy decays at a rate proportional to the cube of the precession frequency.

Sound radiation due to superfluid vortex reconnection was also studied by [43] using the GP equation. The wave energy is first emitted in the form of a rarefaction pulse, which evolves into sound waves. Vortex reconnection in superfluid turbulence was studied first by [54]. During the evolution of a vortex tangle, it is found that the total kinetic energy decreases and the total sound energy increases in the system of energy conservation. In the dynamics of energy cascade of Kolmogorov turbulence, Kelvin waves are excited on vortex filaments and a nonlinear wave dynamics transfers energy from modes of low wave numbers to modes of higher wave numbers (and *vice versa*). Then, since the rate of sound radiation is proportional to the cube of frequency, the sound emission becomes an efficient mechanism of decay of turbulence kinetic energy in the conservative system [60].

Generation of sound by accelerating vortices considered in the preceding sections works in superfluid as well. Barenghi *et al.*[4] investigated a superfluid vortex pair (as a two-dimensional problem) interacting with an isolated vortex filament. The pair changes its direction of motion by close encounter and emits a ripple of sound waves. After the interaction, its kinetic energy  $W$  reduced by the sound emission. Correspondingly, the separation distance  $d$  between the vortices in the pair decreased (since  $W$  is proportional to  $\log d$ , theoretically).

## 9. SUMMARY

On the basis of the theory of aerodynamic sound, studies of vortex sound have been reviewed in this article, focusing on systems of vortex rings and those susceptible of experimental tests, and also on recent new successful areas of computational aeroacoustics and vortex sound in superfluid.

First, the *theory of vortex sound* is reviewed, in particular, on the formulation by multipole expansions. Then, several cases of sound generation by vortex motions are considered, and theories are compared with experimental observations and direct computer simulations. The systems described are, (i) head-on collision of two vortex rings, (ii) oblique collision of two vortex rings, (iii) vortex-cylinder interaction, (iv) a cylinder in a uniform viscous flow, (v) vortex-edge interaction. Comparison between theory and observations shows excellence of the theoretical predictions.

Scaling laws of the pressure of emitted sound are predicted by the theory and compared with experimental observations. Figure 13 is a summary of the experimental scaling laws (by *log-log* plot) for the acoustic pressure amplitude  $\Delta p$  *versus* the translation velocity  $U$  of a single vortex (in isolated state). Observed scaling laws are (a)  $\Delta p \propto U^4$  (head-on collision), (b)  $\Delta p \propto U^{3.2}$  (vortex *vs.* a cylinder), (c)  $\Delta p \propto U^{2.5}$  (vortex *vs.* an edged semi-infinite plate), and (d)  $\Delta p \propto U^{3.3}$  (vortex *vs.* a finite-width

---

<sup>4</sup>The notation (2+1) means that the system is 2D-like but with an additional dimension.

edged plate). Experimental data of each case are shown in Appendix B. Compare these with the predicted laws (51), (72) and (92).

The experimental data served an essential role to test the reliability of the computation codes by comparing computationally generated data with the observed signals. This enables a research area of computational aeroacoustics. Another new aspect is the recent development of study of superfluidity of atomic Bose-Einstein condensates, in which quantized vortices are supported. It is found that sound waves are emitted by accelerating motions of quantum vortices.

## ACKNOWLEDGEMENT

The author is grateful to the editor for giving him an opportunity to review this fascinating and developing area of *Vortex Sound*. He is also indebted to the referees. Owing to their comments, the manuscript has been improved significantly.

## APPENDIX

### A. Nonlinear mechanism of generation of longitudinal components

Acoustic waves are excited by a nonlinear mechanism. Suppose that the initial velocity field is represented by the following Fourier integral:

$$v_i(\mathbf{x}, 0) = \int \hat{v}_i(\mathbf{k}, 0) e^{i\mathbf{k} \cdot \mathbf{x}} d^3\mathbf{k},$$

where  $\mathbf{k} = (k_i)$  is the wave number, and that the velocity field  $\mathbf{v}(\mathbf{x}, 0)$  is solenoidal with satisfying the divergence-free condition:  $\text{div } \mathbf{v} = 0$ , namely  $\mathbf{k} \cdot \hat{\mathbf{v}}(\mathbf{k}) = 0$  at  $t = 0$ . Even if this initial state is satisfied, longitudinal components (with  $\mathbf{k} \cdot \hat{\mathbf{v}}(\mathbf{k}, t) \neq 0$ ) are excited at subsequent times ( $t > 0$ ) by the equation of aerodynamic sound.

Consider the equation (85) of aerodynamic sound for inviscid flows at low Mach numbers:  $(c^{-2} \partial_t^2 - \nabla^2)p = p_0 \partial_i \partial_j (v_i v_j)$ . The source is given by the right hand side, where

$$\begin{aligned} \partial_i \partial_j (v_i v_j) &= \partial_i \partial_j \int \hat{v}_i(\mathbf{k}_1) e^{i\mathbf{k}_1 \cdot \mathbf{x}} d^3\mathbf{k}_1 \cdot \int \hat{v}_j(\mathbf{k}_2) e^{i\mathbf{k}_2 \cdot \mathbf{x}} d^3\mathbf{k}_2 \\ &= - \iint (\mathbf{K} \cdot \hat{\mathbf{v}}(\mathbf{k}_1)) (\mathbf{K} \cdot \hat{\mathbf{v}}(\mathbf{k}_2)) e^{i\mathbf{K} \cdot \mathbf{x}} d^3\mathbf{k}_1 d^3\mathbf{k}_2. \end{aligned}$$

with  $\mathbf{K} = \mathbf{k}_1 + \mathbf{k}_2$ . Assuming the solenoidal property  $\mathbf{k} \cdot \hat{\mathbf{v}}(\mathbf{k}) = 0$ , the coefficient is given by  $(\mathbf{k}_2 \cdot \hat{\mathbf{v}}(\mathbf{k}_1)) (\mathbf{k}_1 \cdot \hat{\mathbf{v}}(\mathbf{k}_2))$  which is nonzero in generic cases. This becomes a wave source for the wave equation (85), even if the initial field was solenoidal.

### B. Experimental data of Fig. 13

The velocity  $U$  denotes the translation velocity of a vortex ring in a single isolated state with the ring radius  $R_0 = 4.7\text{mm}$ . Wave signals were detected at a distance  $r$  from an origin (noted in each case). Experimental data are as follows. The items (a) - (d) below correspond to those in the summary (section 9).

(a)  $r = 630\text{mm}$  from the origin located at the center of collision of two vortex rings. [45];

- (b)  $r = 626\text{mm}$  from the origin located at the center of circular cylinder of radius  $a_c = 4.5\text{mm}$ . The distance of closest approach between the vortex center and the center of the cylinder was  $L = 13.2\text{mm}$ . [46];
- (c)  $r = 634\text{mm}$  from the origin located at the edge of closest approach with the closest distance of the vortex center being  $L = 9.6\text{mm}$ . [33];
- (d)  $r = 632\text{mm}$  from the origin located at the center of edge-line with the closest distance of the vortex center being  $L = 14\text{mm}$ . [48]

## REFERENCES

- [1] Adachi, S., Ishii, K. and Kambe, T. (1997), “Vortex sound associated with vortexline reconnection in oblique collision of two vortex rings”, *Z. Angew. Math. Mech.*, **77**, pp. 716–719.
- [2] Anderson, B.P., Haljan, Regal, C.A., Feder, D.L., Collins, L.A. Clark, C.W. and Cornell, E.A. (2001) “Watching dark solitons decay into vortex rings in a Bose-Einstein condensate”, *Phys. Rev. Lett.* **86**, pp. 2926–2929.
- [3] Batchelor, G.K. (1967) *An Introduction to Fluid Dynamics*, Cambridge Univ. Press.
- [4] Barenghi, C.F., Parker, N.G., Proukakis, N.P. and Adams, C.S. (2005) “Decay of quantized vorticity by sound emission”, *J. Low Temp. Phys.* **138**, pp. 629–634.
- [5] Colonius, T. and Lele, S.K. (2004) “Computational aeroacoustics: progress on nonlinear problems of sound generation”, *Progr. in Aerospace Sci.*, **40**, 345–416.
- [6] Crighton, D.G. and Leppington, F.G. (1970) “Scattering of aerodynamic noise by a semi-infinite compliant plate” *J. Fluid Mech.* **43**, 721–736.
- [7] Crighton, D.G. and Leppington, F.G. (1971) “On the scattering of noise generation”, *J. Fluid Mech.* **46**, 577–597.
- [8] Crighton, D.G. (1972) “Radiation from vortex filament motion near a half plane” *J. Fluid Mech.* **51**, 357–362.
- [9] Crighton, D.G. (1975) “Basic principles of aerodynamic noise generation”, *Aerospace Sci.* **16**, 31–96.
- [10] Crow, S.C. (1970) “Aerodynamic sound emission as a singular perturbation problem”, *Studies in Appl. Math.* **49**, 21–44.
- [11] Curle, N. (1955) “The influence of solid boundaries upon aerodynamic sound”, *Proc. R. Soc. Lond. A* **231**, 505–514.
- [12] Donnelly, R. J. (1991) *Quantized Vortices in Helium II*, Cambridge Univ. Press.
- [13] Ffowcs-Williams, J.E. and Hall L.H. (1970) “Aerodynamic sound generation by turbulent flow in the vicinity of a scattering half-plane”, *J. Fluid Mech.* **40**, pp. 657–670.
- [14] Ffowcs-Williams, J.E. (1969) “Hydrodynamic noise”, *Ann. Rev. Fluid Mech.* **1**, 197.
- [15] Goldstein, M.E. (1976), *Aeroacoustics*, McGraw-Hill.
- [16] Hatakeyama, N. and Inoue, O. (2004) “A novel application of Curie’s acoustic analogy to Aeoliantones in two dimensions”, *Phys. Fluids* **16**, 1297–1304.

- [17] Howe, M.S. (1975) “The generation of sound by aerodynamic sources in an inhomogeneous steady flow”, *J. Fluid Mech.* **67**, 579–610.
- [18] Howe, M.S. (1975) “Contributions to the theory of aerodynamic sound”, *J. Fluid Mech.* **71**, pp. 625–973.
- [19] Howe, M.S. (1998), *Acoustics of Fluid-Structure Interactions*, Cambr. Univ. Press.
- [20] Howe, M.S. (2003), *Theory of vortex sound*, Cambr. Univ. Press.
- [21] Howe, M.S. (2008), “Rayleigh lecture 2007: Flow-surface interaction noise”, *J. Sound & Vib.* **314**, pp. 113–146.
- [22] Ishii, K., Adachi, S. and Kambe, T. (1998). “Sound generation in oblique collision of two vortex rings”, *J. Phys. Soc. Japan*, **67**, pp. 2306–2314.
- [23] Inoue, O, Hattori, Y and Sasaki T, (2000) “Sound generation by coaxial collision of two vortex rings”, *J. Fluid Mech.* **424**, 327–365.
- [24] Inoue, O, and Hatakeyama, N. (2002) “Sound generation by a two-dimensional circular cylinder in a uniform flow”, *J. Fluid Mech.* **471**, 285–314.
- [25] Jordan, P. and Gervais, Y. (2008) “Subsonic jet aeroacoustics: associating experiment, modeling and simulation”, *Exp. Fluids* **44**, 1–21.
- [26] Kambe, T. (1986) “Acoustic emissions by vortex motions”, *J. Fluid Mech.* **173**, pp. 643–666.
- [27] Kambe, T (1993) “Aerodynamic sound associated with vortex motions: Observation and computation”, *Theoretical and Applied Mechanics* (Proc. of the XVIII-th ICTAM, 1992, eds: S.R. Bodner, J. Singer & A. Solan, Elsevier), pp. 239–255 .
- [28] Kambe, T. (2007), *Elementary Fluid Mechanics*, World Scientific Pub. Co. (Singapore).
- [29] Kopiev, V.F. and Chernyshev, S.A. (1997) “Vortex ring eigen-oscillations as a source of sound”, *J. Fluid Mech.* **341**, pp. 19–57.
- [30] Kopiev, V.F. and Chernyshev, S.A. (2000) “Vortex ring oscillations, the development of turbulence in vortex rings and generation of sound”, *Physics - Uspekhi*, **43**, 663–690.
- [31] Kambe, T. and Minota, T. (1981) “Sound radiation from vortex systems”, *J. Sound & Vib.* **74**, pp. 61–72.
- [32] Kambe, T. and Minota, T. (1983) “Acoustic wave radiated by head-on collision of two vortex rings”, *Proc. R. Soc. Lond. A* **386**, pp. 277–308.
- [33] Kambe, T., Minota, T. and Ikushima, Y. (1985) “Acoustic wave emitted by a vortex ring passing near the edge of a half-plane”, *J. Fluid Mech.* **155**, pp. 77–103.
- [34] Kambe, T. Minota, T. and Takaoka, M. (1993) “Oblique collision of two vortex rings and its acoustic emission”, *Phys. Rev. E* **48**, pp. 1866–1881.
- [35] Kopiev, V.F. and Chernyshev, S.A. (2000) “Vortex ring oscillations, the development of turbulence in vortex rings and generation of sound”, *Physics – Uspekhi*, **43**, 663–690.

- [36] Kopiev, V.F. and Chernyshev, S.A. (1997) "Vortex ring eigen-oscillation as a source of sound", *J. Fluid Mech.* **341**, 19–57.
- [37] Lundh E. and Ao, P. (2000) "Hydrodynamic approach to vortex lifetimes in trapped Bose condensates", *Phys. Rev. A*, **61**, 063612.
- [38] Lauvstad, V. R. (1968) "On non-uniform Mach number expansions of the Navier-Stokes equations and its relation to aerodynamically generated sound", *J. Sound and Vib.* **7**, 90–105.
- [39] Lesser, M.B. and Crighton, D.G. (1971) "Physical acoustics and the method of matched asymptotic expansions", *Physical Acoustics* **11**, 69–149.
- [40] Lele, S. K. (1992) "Compact finite difference schemes with spectral-like resolution", *J. Comput. Phys.* **103**, pp. 16–42.
- [41] Lele, S. K. (1997) "Computational Aeroacoustics: A Review", AIAA paper, 97-0018.
- [42] Lighthill, M.J. (1952) "On sound generated aerodynamically. I", *Proc. R. Soc. Lond. A* **211**, pp. 564–587.
- [43] Leadbeater, M, Winiecki, T, Samuels, D.C., Barenghi, C.F. and Adams, C.S. (2001) "Sound emission due to superfluid vortex reconnection", *Phys. Rev. Lett.* **86**, pp. 1410–1413.
- [44] Matthews, M.R., Anderson, B.P., Haljan, P.C., Hall, D.S., Wieman, C.E. and Cornell, E.A. (1999) "Vortices in a Bose-Einstein condensate", *Phys. Rev. Lett.* **83**, pp. 2498–2501.
- [45] Minota, T. and Kambe, T. (1986) "Observation of acoustic emission from head-on collision of two vortex rings", *J. Sound & Vib.* **111**, pp. 51–59.
- [46] Minota, T. and Kambe, T. (1987) "Acoustic waves emitted by a vortex ring passing near a circular cylinder", *J. Sound & Vib.* **119**, pp. 509–528.
- [47] Minota, T., Kambe, T. and Murakami, T. (1988) "Acoustic emission from interaction of a vortex with a sphere", *Fluid Dyn. Res.* **3**, pp. 357–362.
- [48] Minota, T., Murakami, T. and Kambe, T. (1988) "Acoustic waves emitted by a vortex ring passing near a wedge-like plate", *Fluid Dyn. Res.* **4**, pp. 57–71.
- [49] Minota, T., Nishida, M. and Lee, M.G. (1998) "Head-on collision of two compressible vortex rings", *Fluid Dyn. Res.* **22**, pp. 43–60.
- [50] Morfey, C.L. (1976) "Sound radiation due to unsteady dissipation in turbulent flows", *J. Sound & Vib.* **48**, pp. 95–111.
- [51] Möhring, W. (1978) "On vortex sound at low Mach number", *J. Fluid Mech.* **85**, pp. 685–691.
- [52] Nakashima, Y. (2008) "Sound generation by head-on and oblique collisions of two vortex rings", *Phys. Fluids* **20**, 056102.
- [53] Nakashima, Y, Hatakeyama, N and Inoue, O, (2007) "Three-dimensional DNS of sound generation by oblique collision of vortex rings", AIAA-paper 2007–3502.

- [54] Nore, C., Abid, M. and Brachet, M.E. (1997) “Kolmogorov turbulence in low-temperature superflows”, *Phys. Rev. Lett.* **78**, pp. 3896–3899.
- [55] Obermeier, F. (1967) “Berechnung aerodynamisch erzeugter Schallfelder mittels der Methode der Matched Asymptotic Expansions”, *Acustica* **18**, pp. 238–240.
- [56] Obermeier, F. (1980) ‘Berechnung aerodynamisch erzeugter Schallfelder mittels der Methode der Matched Asymptotic Expansions’, *J. Sound Vib.* **72**, pp. 39–49.
- [57] Parker, N.G., Proukakis, N.P., Barenghi, C.F. and Adams, C.S. (2004) “Controlled vortex-sound interactions in atomic Bose-Einstein condensates”, *Phys. Rev. Lett.* **92**, 160403.
- [58] Powell, A. (1964) “Theory of vortex sound”, *J. Acoust. Soc. Am.* **36**, pp. 177–195.
- [59] Strouhal (1878) “Über eine besondere Art der Tonerregung”, *Ann. Phys. Chem.* (Wied. Ann. Phys.) **5**, pp. 216–251.
- [60] Vinen W.F. (2001) “Decay of superfluid turbulence at a very low temperature: The radiation of sound from a Kelvin wave on a quantized vortex”, *Phys. Rev. B*, **64**, 134520.
- [61] Wang, M., Freund, J.B. and Lele, S.K. (2006) “Computational prediction of flow-generated sound”, *Annu. Rev. of Fluid Mech.* **38**, 483–512.
- [62] Zaitsev, M. and Kopiev, V.F. (1993) “Mechanism of sound radiation by a turbulent vortex ring”, *Acoust. Phys.* **39**, 562–565.
- [63] Zaitsev, M., Kopiev, V.F., Munin, A.G. and Potokin, A.A. (1990) “Sound radiation by a turbulent vortex ring”, *Sov. Phys. Dokl.* **35**, 488–489.

